AN ABSTRACT OF THE THESIS OF

CONSTANTINE HADJILAMBRINOS for the degree of MASTER OF SCIENCE in MECHANICAL ENGINEERING presented on JUNE 12, 1986

Title: AN EXPERIMENTAL STUDY OF PLANE JETS ISSUING AT VARIOUS ANGLES INTO A CROSS-FLOW

Abstract approved: Redacted for privacy

Dr. James R. Welty

An experimental study of the properties of plane jets issuing at various angles into a cross-flow of air was conducted to obtain information relating to the momentum diffusion properties of the jet flow in order to provide a background for predicting the feasibility of the preswirl concept of the Volumetric Air Heating Receiver, an advanced solar central receiver concept. The properties investigated included the deflection of the jet axis, the decay of velocity along the jet axis, and the determination of similarity characteristics of the jet velocity profiles.

Experiments were carried out for three different jet-to-cross-flow velocity ratios (R = 4.0, 5.1, 6.2) and angles (θ = 90°, 75°, 60°). Hot film anemometry was used to determine velocity magnitudes.

Correlation of the data obtained revealed that the jet axes for the 90 degree angle correlated very well when the non-dimensional spatial coordinates were reduced by R^2 whereas the axes for the 75 and 60 degree angles correlated well when their coordinates were reduced by R. This

suggested that there was a prominence of momentum effects for the smaller angles, as opposed to a prominence of energy (inertia) effects for the normal jet. The decay of excess non-dimentional velocity for all experimental conditions was very well correlated when the non-dimentional natural coordinate (jet axis) was reduced by R, the relationship between the two being very nearly linear with a -0.77 power of s/hR. The velocity profile data obtained proved to be impossible to correlate and no conclusions on velocity profile similarity could be drawn.

The jet axis and velocity decay correlations proved useful in concluding that the preswirl concept for the V.A.H.R. could be feasible given large enough velues of jet velocity ratio and jet orifice apperture, in order, however, to be possible to draw any definite conclusions for the receiver design, a scaled model of the V.A.H.R. would need to be constructed and tested.

AN EXPERIMENTAL STUDY OF PLANE JETS ISSUING AT VARIOUS ANGLES INTO A CROSS-FLOW

by

Constantine Hadjilambrinos

A THESIS

submitted to

Oregon State University

in partial fulfillment of
the requirements for the
degree of
MASTER OF SCIENCE

Completed June 12, 1986

Commencement June 1987

APPROVED:

Redacted for privacy

Professor of Mechanical Engineering in charge of major

Redacted for privacy

Head of Department of Mechanical Engineering

Redacted for privacy

Dean of Graduate School

Date thesis is presented: June 12, 1986

Typed by: Author

TABLE OF CONTENTS

LIST OF FIGURES

NOMENCLATURE

A	cross-sectional area of jet orifice
Cd	drag coefficient for an airfoil or jet
D	diameter of round jet orifice
Deq	equivalent diameter for non-circular jet orifice
h	width (aperture) of jet orifice for plane jet
l	length of jet orifice for plane jet
n	natural coordinate of jet in cross-flow (normal to the jet axis)
P	perimeter of jet orifice
Q	dynamic pressure
Qj	dynamic pressure of jet at the jet exit
Qm	dynamic pressure of cross-flow
R	ratio of jet-to-cross-flow velocity
s	natural jet coordinate, distance along jet axis
V	velocity at a point in the jet flow
Vc	velocity at the jet axis
Vj	velocity of jet at the jet exit
Vm	velocity of cross-flow (mean flow)
x,y	rectangular coordinates, fixed on test section
θ	angle between jet velocity vector at the jet exit and cross-flow velocity vector

AN EXPERIMENTAL STUDY OF PLANE JETS ISSUING AT VARIOUS ANGLES INTO A CROSS-FLOW

1. INTRODUCTION

The process of a jet mixing with a cross-flow has received, and is still receiving, a great deal of attention because it finds wide application in engineering and science. The complexity of the problem, however, has made a general analytical treatment encompassing all possible variations of flow parameters impossible and has resulted in the various researchers approaching it from the point of view dictated by their particular motivating application (Rajaratnam 1976). The particular case of the plane momentum jet in a cross-flow, in spite of the relative simplicity of its analysis, has not been studied extensively because of the lack of motivating practical applications. An application, however, does present itself in the design of the Volumetric Air Heating Receiver (V.A.H.R.).

1.1 V.A.H.R. Concept Description

The Volumetric Air Heating Receiver is an advanced solar central receiver designed to produce high temperature air. The receiver consists of an array of ceramic fins or

fibers arranged in concentric rows around a central manifold. Solar energy is absorbed on the fins or fibers and is used to heat ambient air which is drawn into the receiver by an induced draft fan (Drost 1985). The original concept includes an outer row of reflecting fins, wedge shaped with specular reflecting surfaces; insolation striking the receiver is reflected by them into the receiver, while reflection and reradiaton out of the receiver is prevented (Figure 1.1). A preliminary study (Drost and Eyler 1981) indicated that the V.A.H.R. concept has several advantages when compared to other air heating receiver schemes such as low reflection and reradiation losses, compactness and simplicity of design, and avoidance of large auxiliary power loads. Based on the results of this study, as well as those of a study on air heating receivers funded by the United States Department of Energy (Bird et al. 1982) and a study of complete process heat facilities using air as the working fluid (Delaquil et al. 1983), the volumetric receiver was identified as an attractive concept and a study was funded at the Pacific Northwest Laboratory (Drost 1985).

1.2 V.A.H.R. with Preswirl

During the course of the investigation performed at Oregon State University by M. K. Drost in connection with the P.N.L. study it became apparent that several features of the original V.A.H.R. concept had to be altered. After

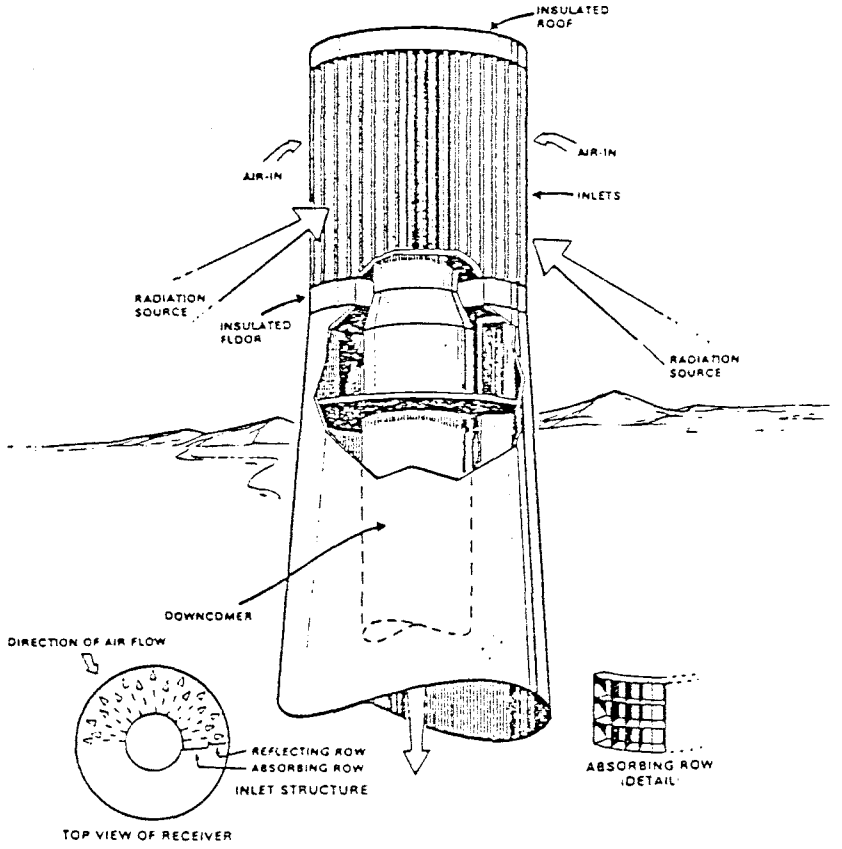

Figure 1.1. Volumetric receiver (Bird et al. 1982)

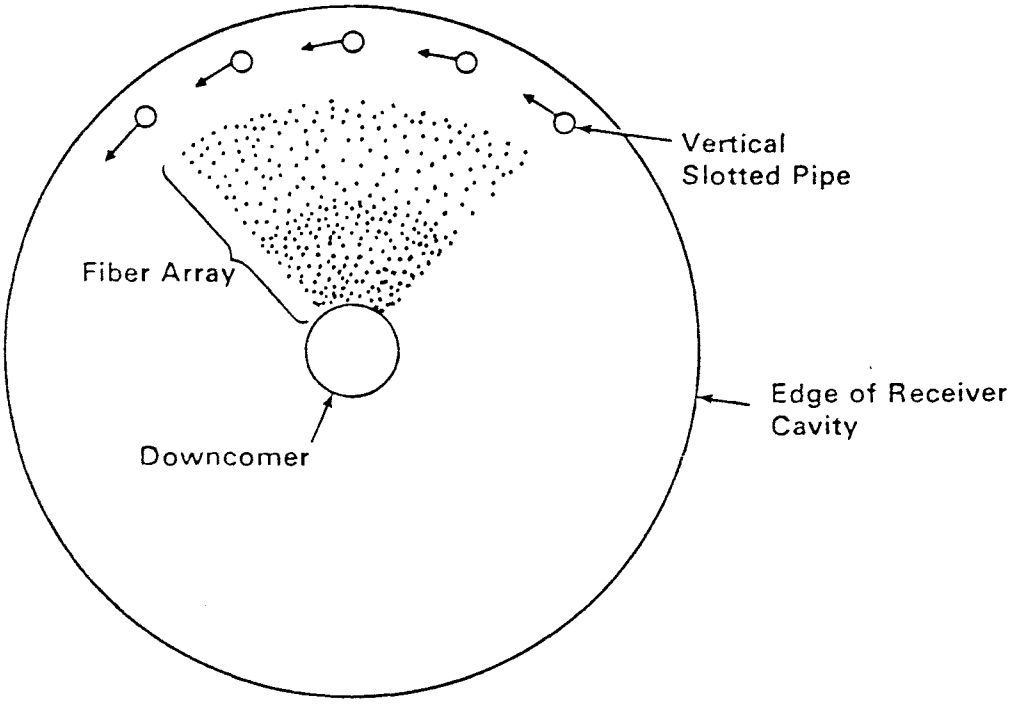

Figure 1.2. Plan View of Preswirl Volumetric Receiver (Drost 1985)

modelling and analysis of the radiation and convective heat transfer in the receiver it became apparent that a fin arrangement would not work because inadequate convective heat transfer would cause overheating of both the reflecting and absorbing fins. In the most attractive design the reflecting fins have been replaced by a shroud for geometric loss reduction, while the absorbing fins have been replaced by cylindrical ceramic fibers for improved convection (Figure 1.2). In spite of these improvements, receiver performance modelling and study suggested that convective heat transfer in the absorbing fiber zone was inadequate and that some convective enhancement method would be necessary. Two convective augmentation methods were considered: 1. rotating a fraction of the absorbing fibers and 2. inducing a free vortex by supplying angular momentum with a series of air jets at the shroud aperture. The free vortex, or preswirl, method was deemed preferable to fiber rotation because of avoidance of structural complications, smaller parasitic energy requirements, and because of induction of the highest velocities past the innermost fibers. The combination of preswirl and small ceramic fibers produced very high convective heat transfer with small parasitic energy consumption, however, because, as a literature search indicated, there is almost no experience in the area of inducing the initial angular velocity (imparting momentum in the tangential direction) by the use of multiple slot jets, there is considerable

uncertainty in the preswirl concept (Drost, 1985). The use of slot jets to induce the preswirl in the volumetric receiver, clearly, provides the motivation for a study of the properties of a planar momentum jet injected into a cross flow.

2. REVIEW OF PERTINENT LITERATURE

2.1 Plane Jets

Both the theoretical and experimental aspects of a plane jet issuing into a still medium (submerged jet) and into a co-flowing stream have been examined over the years. The plane submerged jet is, probably, the simplest jet flow from the analytical point of view. A good mathematical model of this flow is presented by Abramovich (Abramovich 1963). The experimental study, however, of this simple case has presented some difficulties. The results of different investigations undertaken with similar experimental techniques and conditions are found to be in significant disagreement. A possible explanation for this is that the main body of experimentation was done using hot-wire or hot-film anemometry, a method that is inherently laden with large experimental errors because of the high turbulent intensities in the outer regions of the jet flow (Everitt & Robins 1978). The case of a two-dimensional jet discharging into a parallel moving stream does not pose a major problem of experimental accuracy as the velocity in the outer part of the flow no longer tends to zero (ie. is less turbulent) and provides for a good

base case. This flow has a multitude of important characteristics, important because they are common to all jet flows. Both experimental (Bradbury 1965), Bradbury & Riley 1967, Everitt & Robins (1978) and analytical (Abramovich 1963) investigations have recognized three regions common to jet flows, regardless of orifice geometry and existence, magnitude, or direction of a moving medium; an initial or potential core region, a transitional or interaction region, and the main or fully developed region (Fig. 2.1). The initial region is defined as the region in which there is no change in the centerline velocity. The velocity of the potential core (enclosed in this region) remains constant at the value it has at the jet exit. The analysis of this region presented by Abramovich is typical and perhaps the most complete.

The transition region is located between the point where the opposite mixing layers meet (and the potential core ends) and the point where the flow becomes self-preserving or approximately self-preserving. The former point appears to be easily defined and experimental determinations of its location by different investigators have been substantially constant while the latter point is not easily defined. Its position, among other things, appears to be related to the nozzle aspect ratio although it is not clear whether it tends to a constant asymptotic value for large aspect ratios (Everitt & Robins 1978). This region is characterized by interaction between the mixing layers

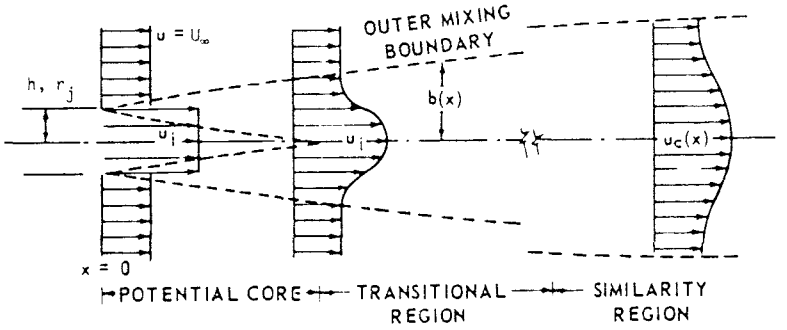

Figure 2.1. Schematic of jet mixing flowfields for the plane jet (Schetz 1980)

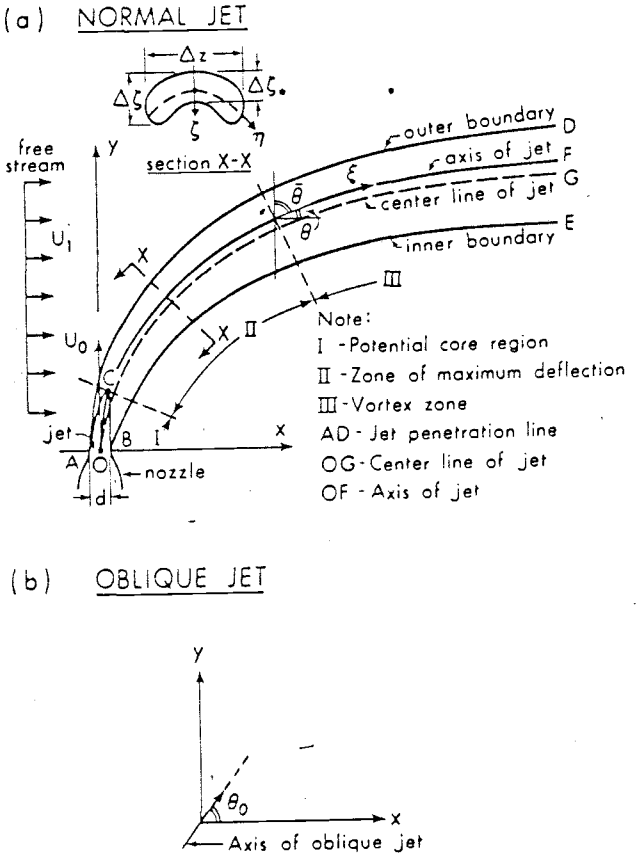

Figure 2.2. Schematic of the circular jet in cross-flow (Rajaratnam 1976)

in which the turbulence structure of each is significatly altered by the other. The analytical modelling for the interaction region is complicated (Abramovich 1963) and it has been ignored in most experimental work with one notable exception (Browne et al. 1984).

The main region of the jet is where the flow becomes fully developed and where self-preservation occurs. The velocity profiles in this region exhibit self similarity (that is for the submerged jet; the jet in a co-flowing stream exhibits only approximate self-similarity). This region is the one that has received the most attention in terms of both mathematical modelling and experimental investigation. An encompassing review of experimental results and analytical approaches has been compiled by Schetz (Schetz 1980) while LDA data recently obtained by Ramparian and Chandrasekhara have been compared with the results of most of the previous researchers (Ramparian & Chandrasekhara 1985).

2.2 Jets in Cross-flow

There are many practical applications where a jet issues at an angle to an external flow such as smokestacks, some fuel injection systems, or the jets in the V/STOL aircraft. In almost all of these cases the jet is injected from a round orifice, or, in some cases, a series of jets is involved injected from a row of round orifices.

Therefore the problem of the round jet in a cross-flow has been the subject of several investigations. Experimental observations have shown that, due to the stagnation pressure exerted by the free stream, the jet gets deflected (Rajaratnam 1976). Depending on the relative strength of the jet to the cross-stream flow, expressed by the ratio, R, of the jet velocity to the free stream velocity, the pressure gradient normal to the jet axis can have a significant effect in the development of the flow. It has been observed that for small values of velocity ratio ($R < 4$) the potential core gets deflected whereas for values of $R > 4$ the streamlines within the potential core remain essentially parallel to the jet direction, the point of termination of the core lies directly over the center of the jet, and jet deflection commences at this point (Keffer & Baines 1963). Keffer and Baines found it convenient to use this point as a virtual origin for plotting the position of the jet in space, to non-dimensionalize the space co-ordinates, dividing them by the jet diameter, and to divide them by the momentum flux ratio R^2 in order to provide a common coordinate system for plotting data. The plot thus obtained indicated a close fit of results (for the jet axis) to a single function with the exception of the results for R=2 and 4. It was also observed that when related to the natural system of axes the flow displays similarity and approximate self-preservation. The main effect of the pressure forces and lateral shear induced by

the cross-flow is to shorten the potential region and to change the shape of the cross-section from circular to a characteristic kidney-shape at the end of the region. Entrainment and acceleration of the surrounding fluid occurs as the jet decelerates. A wake is created behind the jet and two attached vortices appear, exactly as found in flow around a cylinder at low Reynolds number (Pratte & Baines 1967). The mean velocity of the jet decreases much more rapidly than in the free jet and the deflection is strong so that within a relatively short distance the jet is moving in a direction within a few degrees of the main flow. Though the jet strength diminishes rapidly, the strength of the twin vortices lessens much more slowly with the effect that the greater part of the downstream region is primarily characterized by vortex flow. Thus, the round jet in cross-flow can be divided into three zones (Fig. 2.2): the potential zone or core, the zone of maximum deflection (where both jet and vortex flow are important), and the vortex zone (Pratte & Baines 1967). It should be noted that Pratte and Baines prefer the non-dimensionalized coordinates of the type x/DR to those used by Keffer and Baines. A detailed analysis of the "near region" of the jet which includes the potential and maximum deflection zones was done by Moussa, Trischka, and Eskinazi for a rather weak jet ($R < 4$) and the similarity of the flow field around the jet to that around a solid cylinder was re-affirmed (Moussa, Trischka, & Eskinazi 1977). An

experimental investigation of the turbulence characteristics of a weak jet in a cross-flow (R = 2.3 and 1.15) was preformed by Crabb et al. (1981) who have included a summary of a substantial number of previous investigations on the subject.

One important distinction to be made in the study of deflected jets is between the center line and the axis of the jet. Because of the pressure gradient imposed on the jet by the cross-flow, the locus of maximum velocity points (axis of jet) does not coincide with the line defining the half-way points between the edges of the jet (center line), as is the case in the free jet, but lies on the upstream side of the center line, closer to the leading edge. Equations describing the location of both the center line and the axis, as well as the edges of the deflected axisymmetric jet have been proposed by various investigators. Most of these are reviewed by Rajaratnam (1976). Because of the complexity of the flow, the analytically formulated models, generally, are not in as good agreement with experimental observations (which differ significantly among investigators, it must be noted) as the empirical models. A comparison among proposed empirical equations for the axis of the jet suggests the equation proposed by Shandorov (Abramovich 1963) to be preferable for predicting the axis as it is closer to the mean curve produced by combining the equations used by the various investigators for fitting their data (Rajaratnam 1976).

This (Eqn. 1) is reduced from a more general equation, derived for the general case of an oblique jet in cross-flow.

$$y/D = R^{0.79}(x/D)^{0.39} \qquad [1]$$

Equation 2a is written in terms of dynamic pressures, whereas equation 2b is reduced to velocity ratios.

$$x/D = Qm/Qj(y/D)^{2.55} + y/D(1 + Qm/Qj)\cot\theta \qquad [2a]$$

$$x/D = R^2(y/D)^{2.55} + y/D(1 + R^2)\cot\theta \qquad [2b]$$

Shandorov, Ivanov (Abramovich 1963) and Platten and Keffer carried out experiments to determine the trajectories of jets injected into cross-flow at various angles. Platten and Keffer obtained consistent data with little scatter and reached the conclusion that there is no obvious self-similarity of the jet trajectories (Platten & Keffer 1971). It should be noted that Ivanov also experimented with rectangular jets (with side ratios of 5:1 and 1:5) and concluded that, in a first approximation for the axis of a rectangular jet, the equation for the axis of a circular jet may be used with an equivalent diameter. In the limiting case of an infinite plane jet, this value equals twice the thickness of the jet:

$$Deq = 4A/P = 4hl/2(h + l) \longrightarrow 4hl/2l = 2h \qquad [3]$$

2.3 The Plane Jet in Cross-flow

An analytical method for computing the axis of the plane jet in cross-flow was proposed by M. S. Volinskiy (Abramovich 1963); it is based on the condition that the force caused by the pressure difference at the forward and back surfaces of the jet is balanced by a centrifugal force caused by the jet's change in direction. The method assumes that the deflected jet acts as a solid surface against the cross-flow and a resistance coefficient C_d can be assumed, the value of which, as known by experimental aerodynamics, is of the order of magnitude of 1. This method was slighly modified by Abramovich who based his calculations on the assumption that the component of the total momentum of the jet perpendicular to the direction of the cross-flow remains constant. Equation 4, the axis equation for a plane jet, was obtained for the conditions of constant cross-flow density and velocity (Abramovich 1963).

$$k(y/h) = 2\ [\ \pm\sqrt{k(x/h) + \cot^2\theta}\ -\ \cot\theta] \qquad [4]$$

$$k = C_d/(R^2\sin^2\theta)$$

When this equation is applied to the air curtain problem, it becomes apparent that C_d cannot be constant for different jet injection angles. The determination of the appropriate value for C_d must be done experimentally.

Experiments on plane jets in cross-flow have been conducted by Girshovich (Girshovich 1966) for $\Theta = 90^{\circ}$ and R from 2.5 to about 10, and by Choi and Wood (Choi & Wood 1966) for $\Theta = 9^{\circ}$, 17° and 25° and R varying from 2.6 to 9.0. Choi and Wood have shown that the distribution of the dynamic pressure normal to the s-axis (Fig. 2.3) is similar for the various injection angles and velocity ratios (Fig. 2.4). The growth rates of the jet on either side of the jet axis (s coordinate) were found to be unequal and the growth of the total width with s was not linear. The decrease of the dimensionless dynamic pressure excess on the jet axis varied almost linearly with 1/s and while for the smaller angles the profiles of the axis are well correlated by the coordinate system $y/(R^2h)$ versus $x/(R^2h)$, this is not true for large injection angles (ie. the jet axis is not independent of the velocity ratio even when the length scales were divided by R^2).

Analytical solutions for both the main and initial regions of the plane jet in cross-flow have been developed by Girshovich (Girshovich 1966, a & b). The solution for the main region is based on the following assumptions: 1) the jet issues from an infinitely thin slot; 2) the velocity and pressure on the outer edge of the jet are equal to the velocity and pressure obtained for flow past a solid wall having the same shape as the axis of the jet; 3) the velocity is equal to zero and the static pressure is constant on the inner edge (this assumption is not valid

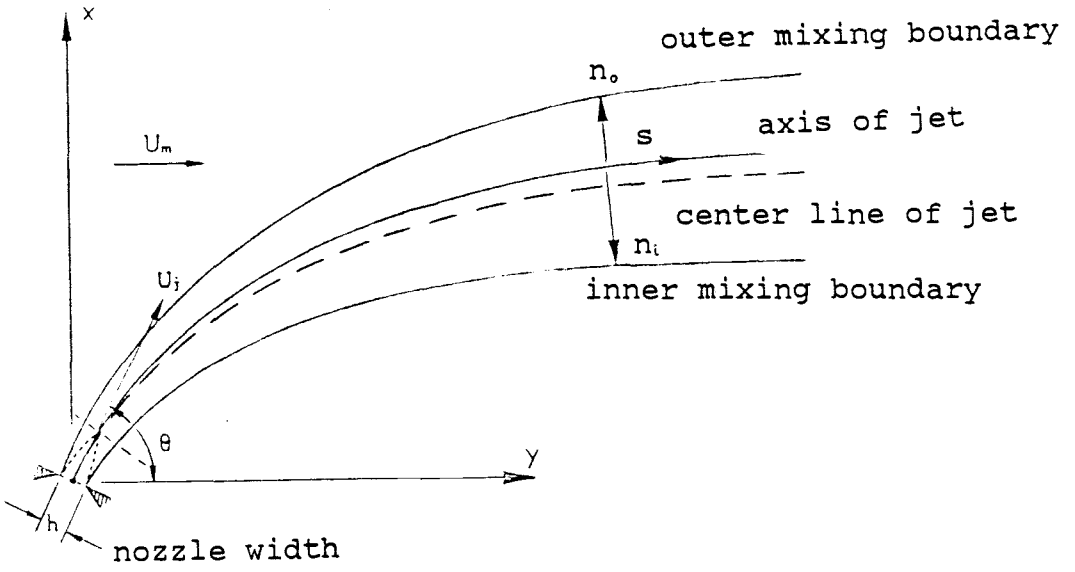

Figure 2.3. Schematic of the plane jet in cross-flow

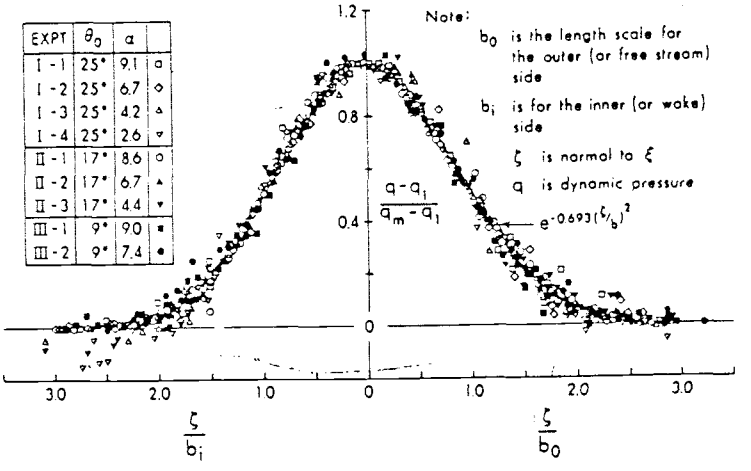

Figure 2.4. Dimensionless excess dynamic pressure profiles for plane jets in cross-flow (Choi & Wood 1966)

for jets issuing at either very small, $\theta << 90°$, or very large, $\theta >> 90°$, angles and for distances far from the exit); 4) the jet axis is a streamline; 5) the tangential stresses are equal to zero on the axis; and 6) the mixing length is constant across the axis. From these, equations are obtained for the relative profile of the non-dimensional velocity distribution, for the inner and outer jet edges, and for the jet axis. The solution for the initial segment is solved for a jet issuing at right angles to the cross-flow. The assumptions for this solution are: 1) the curved axis of the jet is the zero streamline; 2) the radius of curvature of the axis in the initial segment is constant; 3) in the potential core the transverse velocity is considerably less than the longitudinal; 4) in the outer and inner mixing zones, which are separated from one another, the mixing lengths are different and proportional to the width of their respective mixing zones, the coefficient of proportionality being the same; and 5) the velocity profiles across the mixing zones are similar. The assumptions regarding the conditions at the inner and outer edges were the same as for the solution for the main region. The equations obtained for the two regions can be reduced to the equations describing the submerged plane jet. The solutions of these equations (for the jet issuing at right angles to the cross-flow, of course) were combined and compared with experimental data (Girshovich 1966, b). The conclusion drawn by the comparison is that the

theoretical solution satisfactorily describes, both quantitatively and, most importantly, qualitatively the propagation of the plane jet in a cross-flow with the exception being the description of the jet axis. The disagreement between experimental data and theoretical solution was attributed to the failure of the assumption of constant (ie. atmospheric) pressure at the inner edge to take into account the rarefication occuring behind the initial segment of the jet.

3. TEST FACILITIES AND EXPERIMENT

3.1 Test Objective

Three objectives were identified for the experiment: 1) determination of the position of the axis of the deflected jet, 2) determination of the decay of the velocity on the jet axis with distance from the jet orifice, and 3) investigation of the self-preservation properties of the flow. These characteristics of the flow were to be investigated for jets issuing, at various angles and with different velocity ratios, into the cross-flow.

The jet axis, in accordance with previous investigators (Choi & Wood 1966) was defined as the streamline passing through the central vertical line at the (vertical) nozzle exit plane. The only practical way of determining the trajectory of this streamline is by virtue of its property of being the location of maximum velocity occurence at any particular jet length. The jet axis can therefore be determined by plotting the locus of maximum velocity points within the jet flow field. Once the trajectory of the jet axis is determined and the magnitudes of velocity along it are known, the decay of axial velocity

with distance from the jet orifice can be determined. The existence of self-preservation can be verified by determining the velocity profiles at various locations in the jet and checking their similarity. Measurments of the velocity at various points within the flow field could, therefore, accomplish the experimental objectives.

3.2 Apparatus and Instrumentation

The experiments were conducted in a wind tunnel located in Graf Hall on the Oregon State University campus. The wind tunnel is shown in Figure 3.1. The test section located on top of the plenum chamber was modified to accomodate the experiment. The main flow of air was produced in this 2 ft x 4 ft x 5.5 ft test section by a centrifugal and an axial flow fan. The flow was controlled by the plug located in the plenum chamber. A honeycomb flow straightener along with five wire mesh screens, followed by a converging section at the inlet were used to reduce turbulence.

The jet flow was produced by a specially constructed jet manifold (Fig. 3.2). The manifold consisted of two 1/4 in tubes inside a 1 in square pipe. The tube array was designed so that it could be inserted into the square pipe with one end providing a slip-fit and the other end being threaded in order to make tightening possible. This design facilitated installation into and removal from the wind

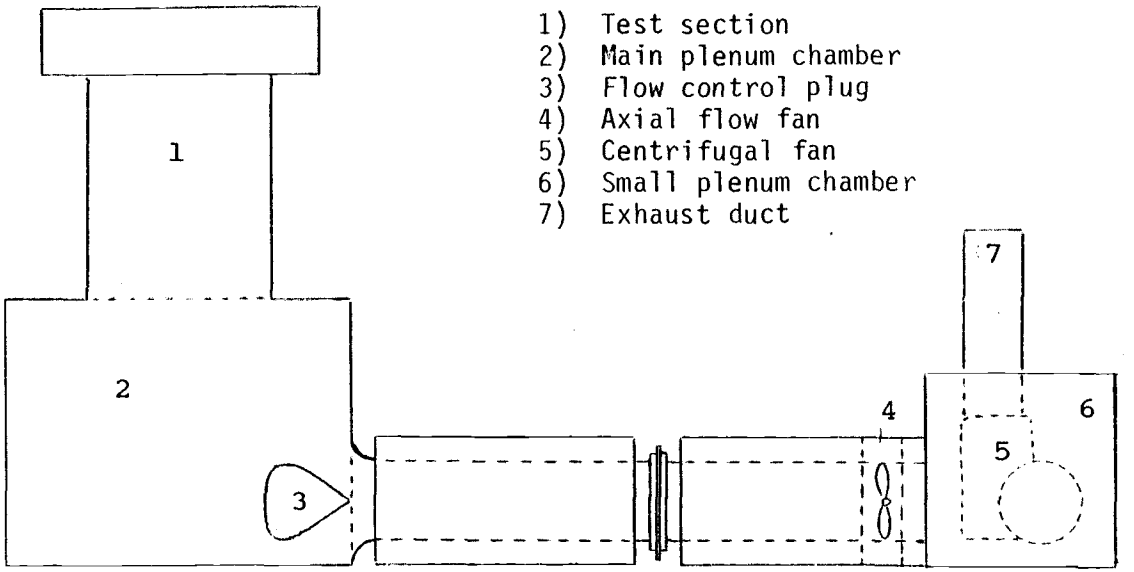

Figure 3.1. Wind tunnel layout

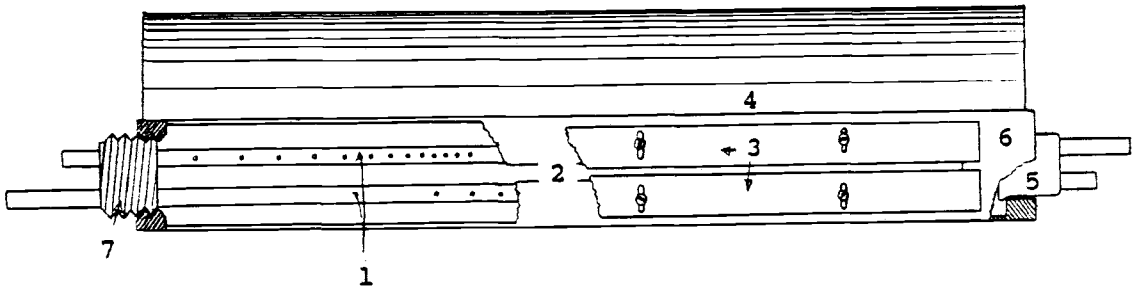

1) 1/4 in tube array
2) Jet slot
3) Edge plates
4) Spoiler
5) Slip fit tube array plug
6) Square pipe
7) Threaded tube array plug

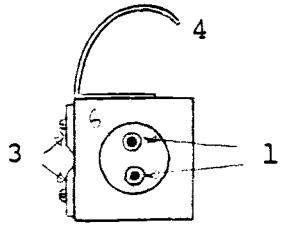

Figure 3.2. Front and side views of jet manifold

tunnel of the jet manifold. A 22 in long slot was cut into one of the sides of the square pipe and two edges were fitted in a way that made adjustment of the width of the jet aperture possible. The edges were metal plate pieces machined to a sharp straight edge along one side and with small slots cut into them enabling them to be screwed onto the manifold side in different positions, opening or closing the jet orifice as needed. A line of round holes were drilled into the 1/4 in tubes the spacing of which (sparse towards the ends, getting closer together towards the center) was designed to produce as nearly a uniform flow distribution along the length of the manifold as possible. The jet flow was produced by air entering the tubes from both ends, exhausting into the square pipe from the rows of holes where it expanded and achieved further pressure uniformity.

Due to its rectangular shape the jet manifold created a disturbance of the main flow. Such a disturbance could have only been avoided if the jet orifice were flush with a wind tunnel wall. This was not done, in order to maintain simplicity of design and approximate the application conditions: the slot jets to be incorporated in the V.A.H.R. design would have to originate from pipes, the presence of which would undoubtedly interfere to some degree with the flow. In order, however, to minimize such interference a "spoiler" (ie. a specially shaped piece of sheet metal) was added to the jet manifold in order to

improve its aerodynamic characteristics.

To install the jet manifold into the wind tunnel the square pipe was held inside the tunnel while the tube array was slid into it through round holes (one in each of the two walls between which the manifold was set) and was screwed tight, the round plugs of the tube array protruding past the pipe ends and setting into the wall holes, thus allowing the manifold to be rotated around its axis. In order to seal the spaces between the tube array plugs and the wall and to provide with a friction fit to prevent the manifold from moving freely, a non-hardening sealing putty, "plastilina" was used. This allowed the manifold to maintain its position while in use while making possible its rotation when a new jet to cross-flow angle setting was desired.

The jet flow was produced by a Gardner reciprocating compressor located in the basement of Graf Hall. The compressed air was carried from the compressor tank to the jet manifold via a 3/4 in rubber hose. A control panel (Fig. 3.3) was constructed to divide the flow in two and control the flow rate into both manifold tubes. Each of the two resulting flows was again divided in two and was directed to the opposite ends of the manifold by Tygon tubing. The reason for the use of two tubes inside the jet manifold was to maintain a uniform flow along the manifold length. Because of their small inside diameter, each tube was incapable of exhausting at a uniform pressure along its

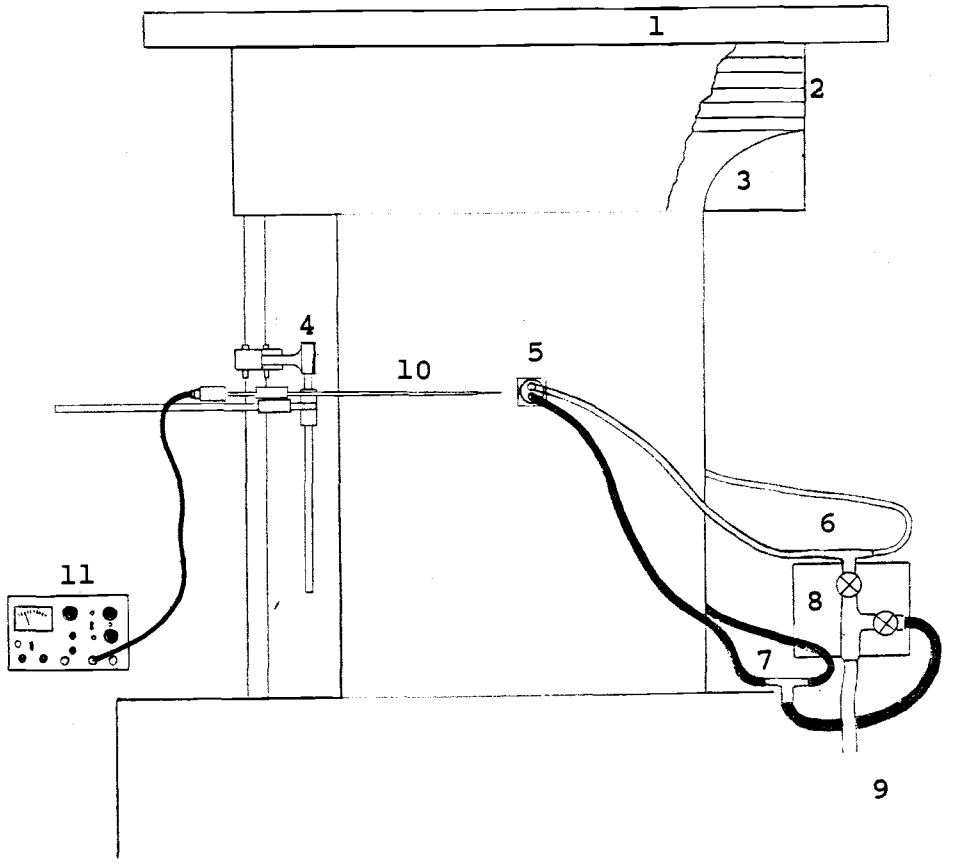

1) Honeycomb flow straightener
2) Wire mesh screens
3) Converging section
4) x-y positioner
5) Jet manifold
6) Tygon tubing to 1/4 in tube 1
7) Tygon tubing to 1/4 in tube 2
8) Flow control panel with valves
9) Flow from compressed air source (Gardner compressor)
10) Probe holder with probe
11) Anemometer

Figure 3.3. View of test section and experimental apparatus

entire length there being a pressure drop in the flow from the two ends, towards the center. If, in order to alleviate this problem, the hole spacing were to be increased, then the pressure equalization taking place inside the jet manifold (ie. outside the tubes but inside the square pipe) would be insufficient to produce a uniform plane jet flow. The two tube array minimized the problem by doubling the available tube cross-sectional area and allowing one tube to provide the flow for the ends of the manifold while the other provided the flow for the central manifold section. Thus, a fairly uniform pressure distribution was maintained. This particular design was prefered over a design incorporating a single tube of a larger diameter because it made the incorporation of a smoke generator for flow visualization easier by allowing for only a portion of the total flow to pass through the smoke generator and lowering the pressure that it would have to handle (to only slightly higher than the pressure inside the jet manifold). The jet manifold had to be re-designed after it became apparent that the smoke generator could not function in a high pressure, the flow visualization portion of the experiment, however, could not be carried out due to lack of time.

Hot film anemometry was used to measure velocities in the flow-field created by the jet and cross-flow. The anemometer system used was manufactured by Thermo-Systems Inc. consisting of a Model 1051-2 Monitor and Power Supply

Module, a Model 1057 Signal Conditioner, a Model 1054A Constant Temperature Linearized Anemometer and a Model 1056 Variable Decade (control resistance).

A variety of anemometer probes were tested and the one with optimal performance characteristics was used. The selected probe was a T.S.I. Model 1212.20 hot film probe. This probe was chosen because it created the least disturbance in regards to both the jet and main (cross) flow, due to its shape, because it offered the best sensitivity to velocity changes (when compared to hot wire probes), and because it was the least affected by velocity directional changes. The probe was calibrated in a velocity range from 3.0 m/s to 76.0 m/s and in a flow direction range from 0 to 90 deg. A typical calibration curve is compared with a hot wire probe calibration curve in Fig. 3.4 and it can be seen that there is a greater response to velocity change of the 1212.20 probe than of the hot wire probe. Figures 3.5a and 3.5b illustrate the fact that hot film probes, in general, show a smaller (and more constant with velocity magnitude change) pitch response than hot wire probes when measuring velocities greater than 1 m/s. In addition to its response advantages, the T.S.I. 1212.20 probe had the advantage of ruggedness and ease of handling.

The probe was positioned in the wind tunnel by a specially constructed X - Y mover with the capability of accurate positioning over a range of 0.6 m in both the X

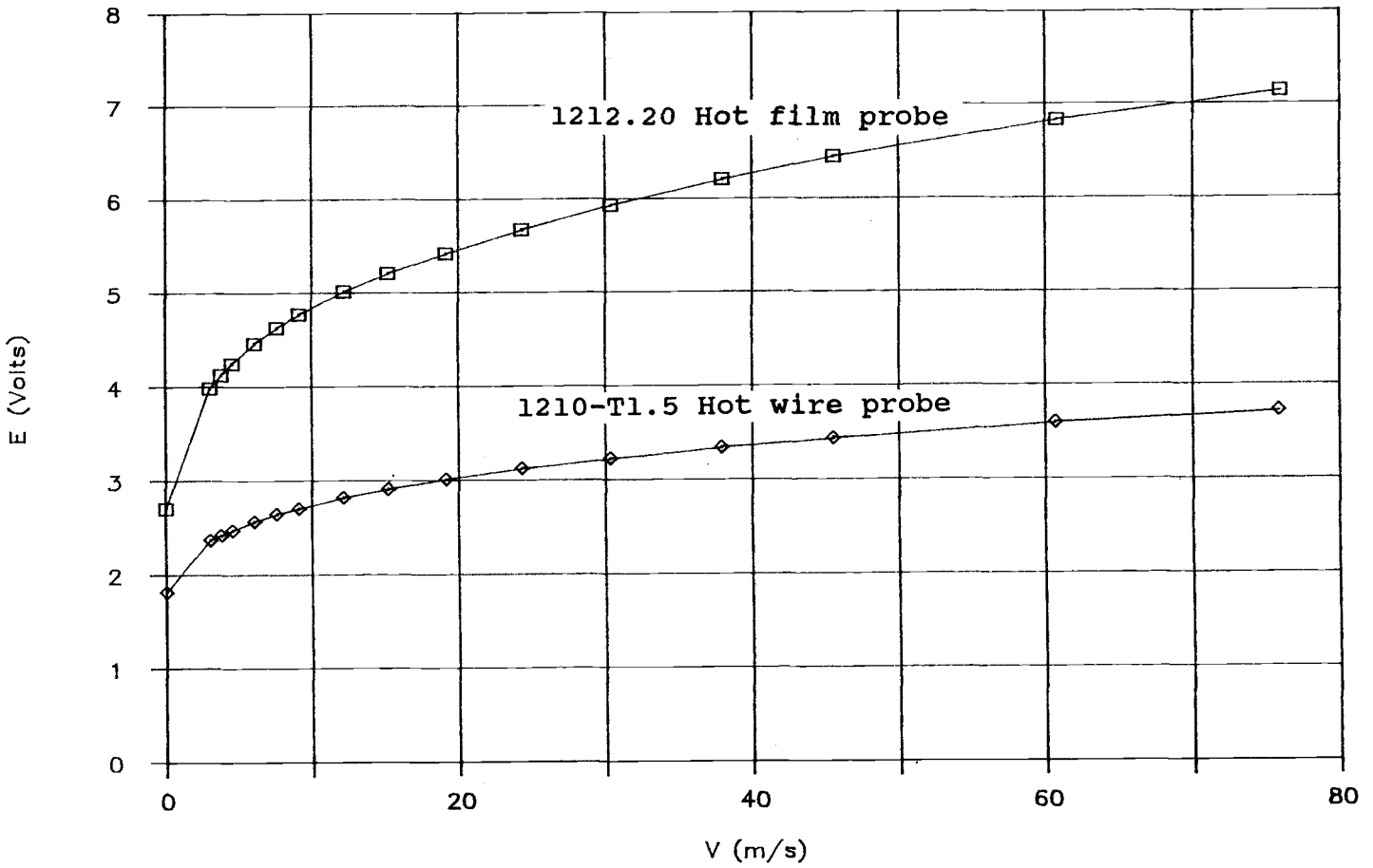

Figure 3.4. Hot wire and hot film anemometer calibration curves

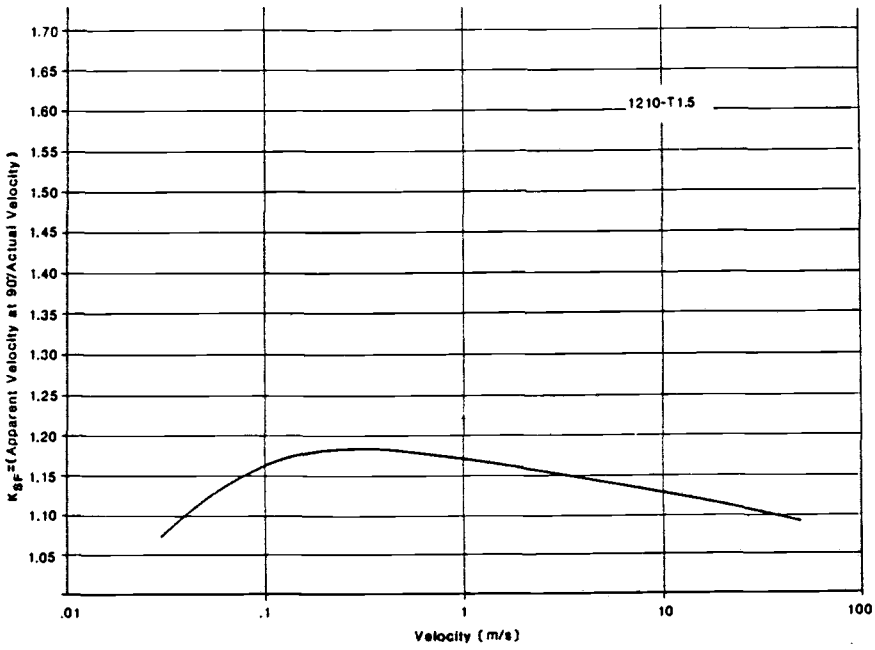

a) 1210-T1.5 Hot wire probe

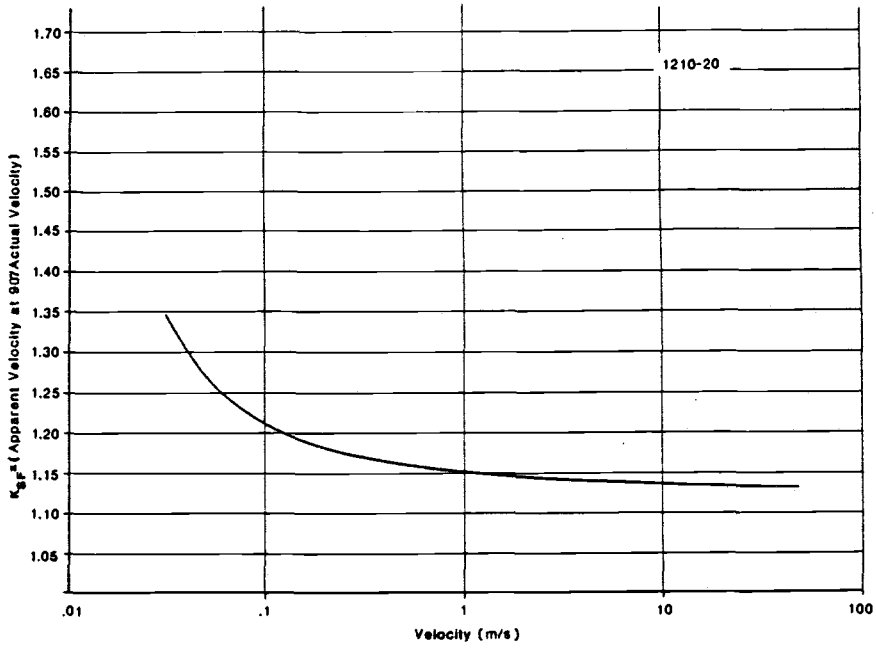

b) 1210.20 Hot film probe

Figure 3.5. Pitch response of typical hot wire hot film probes

and Y directions (Fig. 3.3).

3.3 Experimental Procedure

Before any velocity readings could be taken the hot film probe had to be calibrated. The calibration was done using a T.S.I. Model 1125 Gas Probe Calibrator with an 1125R-1 Probe Rotator which was capable of producing air velocities in the range from 10 ft/s to 250 ft/s (3 m/s to 80 m/s) with an accuracy of $\pm$ 2%. The voltmeter used to determine the probe response (ie. the voltmeter provided on the T.S.I. Power Supply) had a resolution of 0.005 volts which resulted in a velocity uncertainty of $\pm$ 0.6%. Repeated calibrations were performed and an average linearized curve (of the form: $E^2 = aV^{.5} + b$) was obtained and used to transform the voltage readings into velocities. The various calibration curves varied no more than 1%. The integrity of the probe was periodically checked during the course of the experiment by re-calibration and if a change of over 2% was found to have occured in the calibration curve a new set of calibrations (three) were performed and a new average curve was determined.

Before any experiment began, the uniformity of the jet produced by the jet orifice was checked. This was done by moving a Pitot tube along the orifice and measuring the variation in dynamic pressure. The variation in dynamic pressure observed was about 10% for low jet velocities and

decreased to about 5% as the jet velocity increased. Therefore, the variation in jet velocities produced by the jet orifice was determined to be in the range of 3% to 2%, dynamic pressure being a function of the square of velocity.

In order to get a feeling for the interference in the mean flow caused by the jet manifold, a cross-flow of 3 m/s was created with no jet flow, and velocities near the manifold were determined for various positions of the manifold. The conclusion drawn from these measurments was that for the 90 deg. position there was little interference by the jet manifold; a boundary layer was created on the manifold surface resulting in a drop in velocity at small distances from it (up to about 3 mm) and a turbulent wake occurred directly down-stream of the manifold. For positions of the manifold of 75 and 60 deg., an area of stagnant fluid was observed, this area being greater for the smaller angle, extending to a distance of about 10 mm from the jet apperture. Thus for positions other than 90 deg., the manifold would be expected to interfere to some degree with the mixing flow field.

A set of nine experiments was run in a combination of three jet-to-cross-flow angles (90, 75, and 60 deg.) and three jet-to-cross-flow velocity ratios (R = 4.0, 5.1, and 6.2). Velocity readings were taken by traversing the probe in either the x or y direction. The traversing was done by the x-y positioner that had a resolution of 0.1 mm in

either direction.

Because of the limitations of the compressor producing the jet flow, a small aperture of the jet orifice had to be used. The jet width (orifice aperture) used to produce a velocity ratio R = 4.0 was 1 mm while, in order to produce higher velocity ratios, a width of 0.5 mm was used for R = 5.1 and 6.2. The smaller jet width necessitated a finer resolution of spatial coordinates (and a decrease in positioning accuracy), it is, however, eliminated as an experimental variable by non-dimensionalization of the spatial coordinates, dividing them with the jet width (h). For both orifice apertures used, the jet approximated an infinite plane jet by having a large aspect (orifice length to width) ratio (Table 3.1).

Table 3.1

R	h (mm)	Aspect ratio
4.0	1.0	550
5.1	0.5	1100
6.2	0.5	1100

Throughout the experiments ambient conditions (pressure and temperature) were recorded, and the probe readings were adjusted to take into account the air density variations. Since the jet was not heated, no buoyancy effect had to be taken into consideration.

4. RESULTS

The first objective identified at the onset of the experiment was the determination of the trajectories of the jets (ie. the location of the jet axes in x-y space). This was accomplished by velocity measurements in traverses in the x or y direction. In this way the location of maximum velocity points at various distances downstream of the jet orifice was determined. The location of these points for the nine experiments was plotted in the non-dimensional coordinates x/h vs. y/h (Figures 4.1, 4.2, and 4.3). It can clearly be seen from these plots that the deflection of the jet axis is a function of both the velocity ratio, R, and the injection angle, Θ, the greatest deflection occurring at the lowest R and Θ (4.0, and 60 deg.). The data, with few exceptions, fit well into smooth curves, in spite of the relatively high uncertainty of the exact coordinates of the maximum velocity position at the greatest downstream distances. This uncertainty was due to the increasingly flattenned velocity profiles with increasing distance and was the factor determining the greatest distance from the orifice at which reasonable data could be taken.

In order to correlate the experimental results, the jet axes were plotted in the non-dimensional coordinates reduced by the jet-to-cross-flow velocity ratio squared which is the correlation suggested by Abramovich (Abramovich 1963) and adopted by various other investigators of round jets in cross-flow (Keffer and Baines 1963) and plane jets in cross-flow (Choi and Wood 1966). The R^2 correlation is indicative of a prominence of kinetic energy (inertia) effects and appears to work well for $\theta = 90°$. The Volinskiy-Abramovich model (Eqn. 4) is also plotted with the data and it too seems to be well correlated with the $\theta = 90°$ data (Fig. 4.4). The inertia correlation and the Volinskiy-Abramovich equation however, do not hold well for the 75 and 60 deg. angle data (Fig. 4.5, 4.6). The division by R^2 is, in these cases, over-compensated by reducing the higher velocity ratio data, consistently, to a greater degree. This trend is present even in the $\theta = 90$ deg. case to a lesser extent, suggesting a correlation of a power of R less than 2. In regards to the Volinskiy-Abramovich model, it should be noted that an adjustment of the origin by values of approximately 0.2 in the reduced coordinates was used, taking into account the potential core region length, in which the jet axis is not deflected by the cross-flow. In addition to this, drag coefficient (C_d) values between 3 and 4 were used, exceeding the suggested range $1 < C_d < 3$. This, however can readily be justified by the fact that the jet flow does

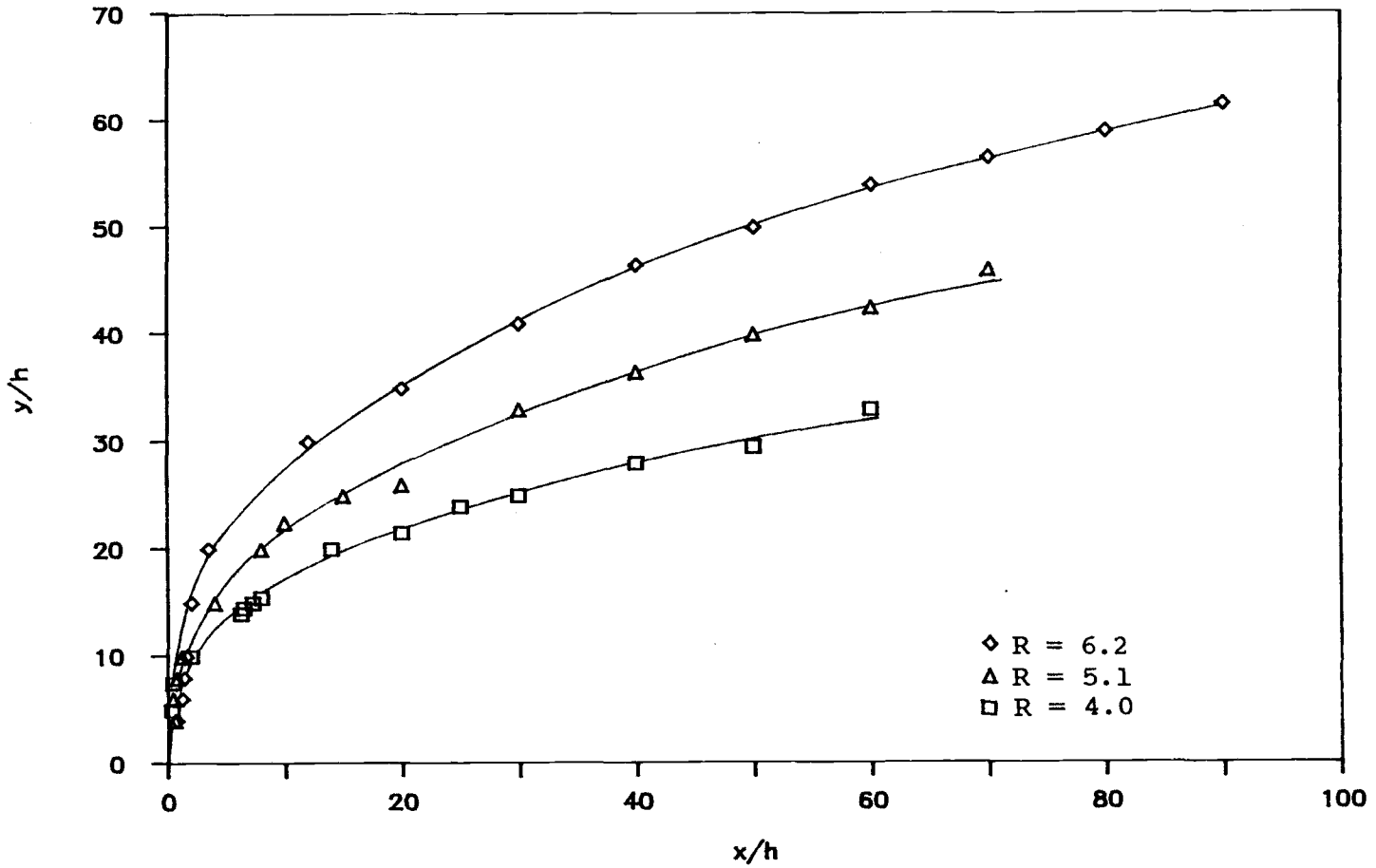

Figure 4.1. Location of jet axes for $\Theta = 90^{\circ}$

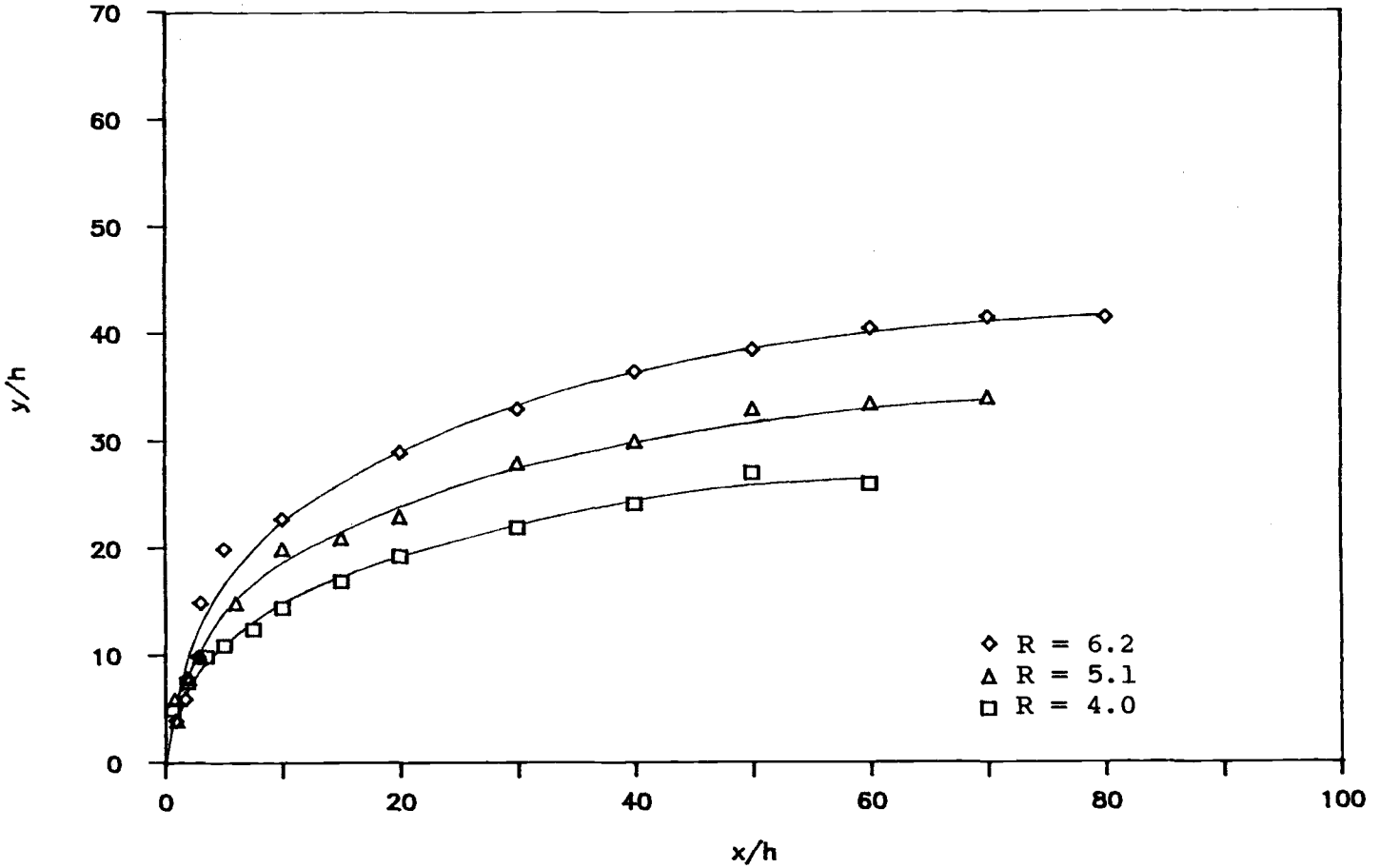

Figure 4.2. Location of jet axes for $\Theta = 75^{\circ}$

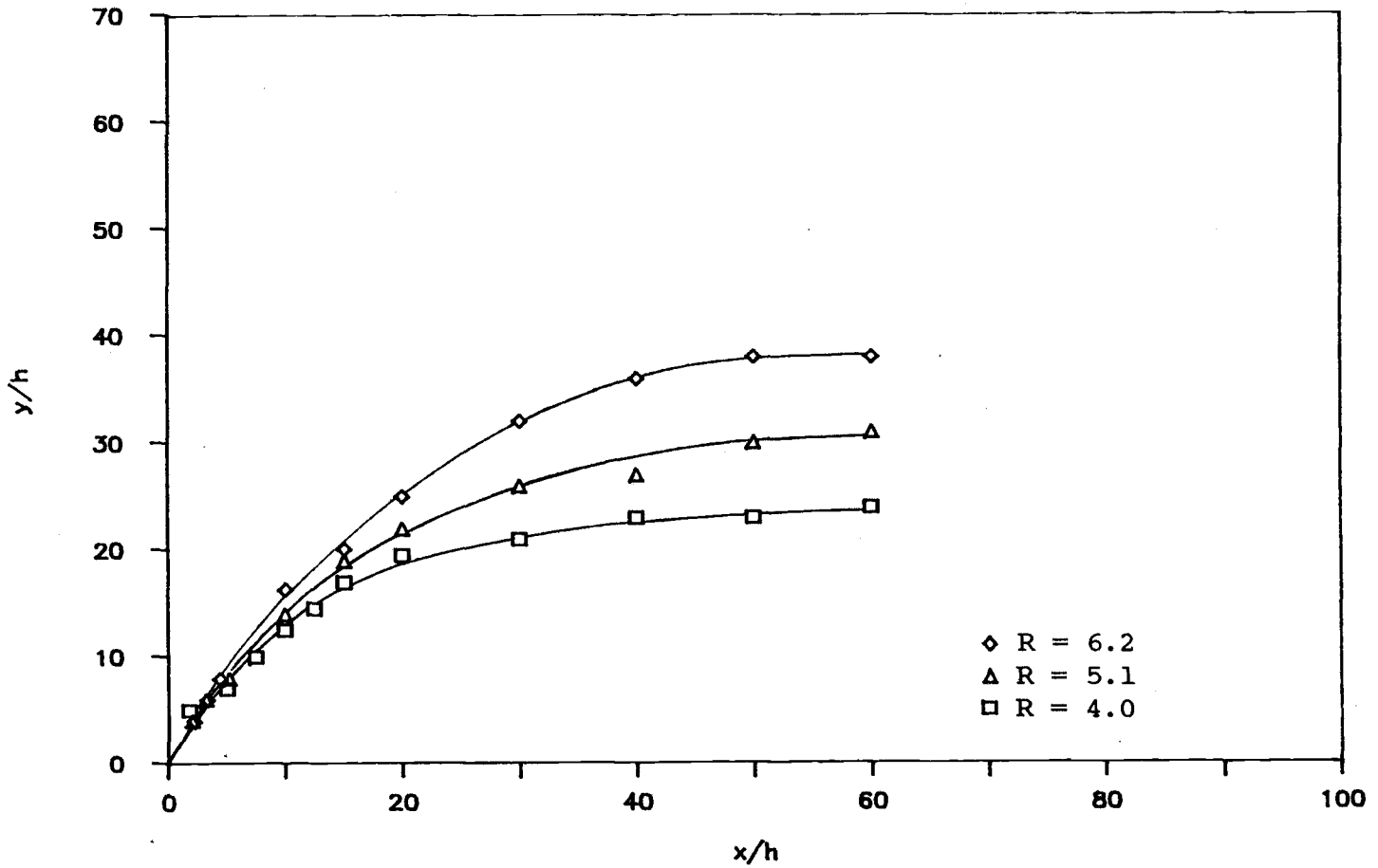

Figure 4.3. Location of jet axes for $\Theta = 60^{\circ}$

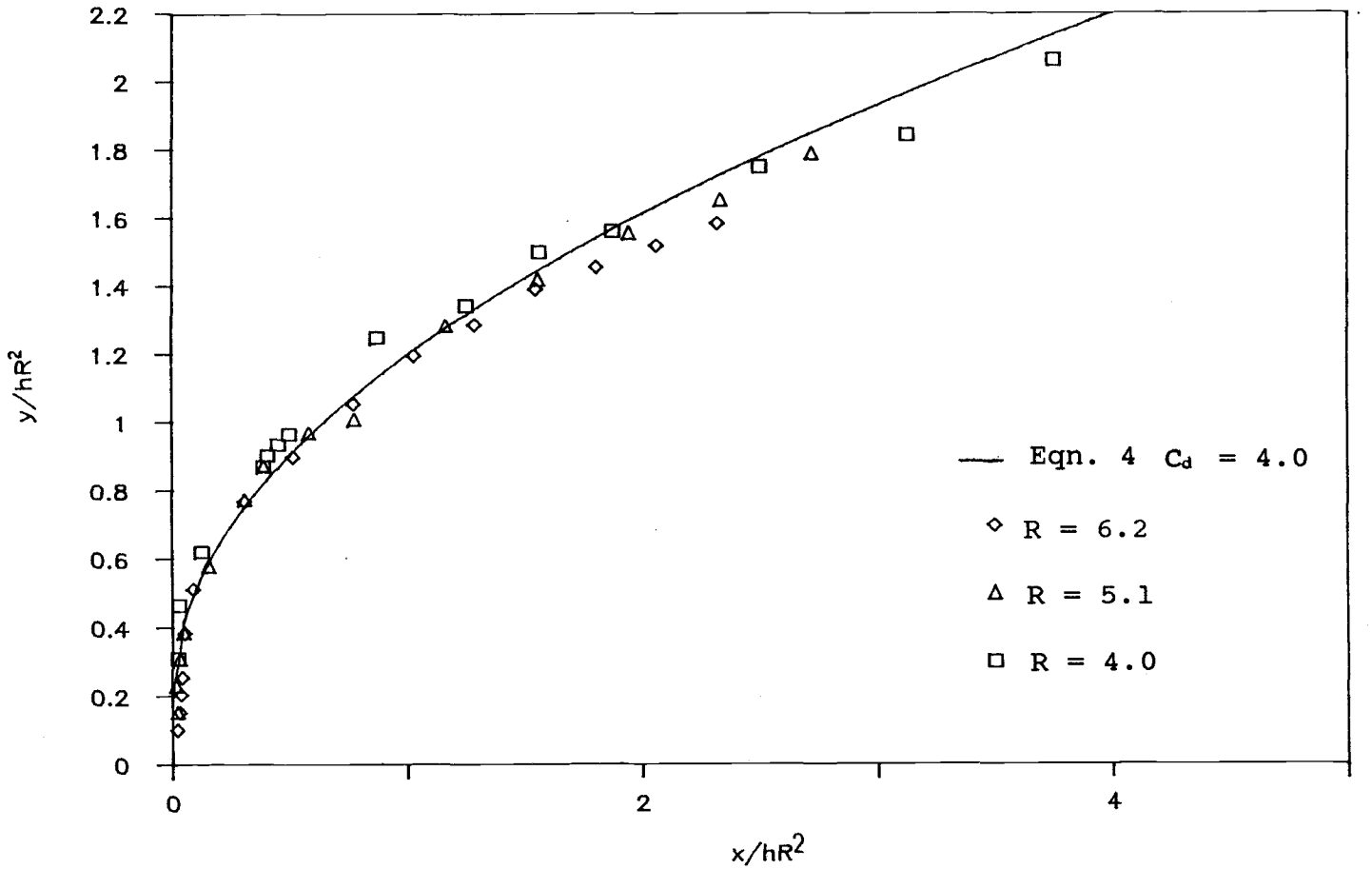

Figure 4.4. Jet axes reduced by R^2 for $\Theta = 90°$

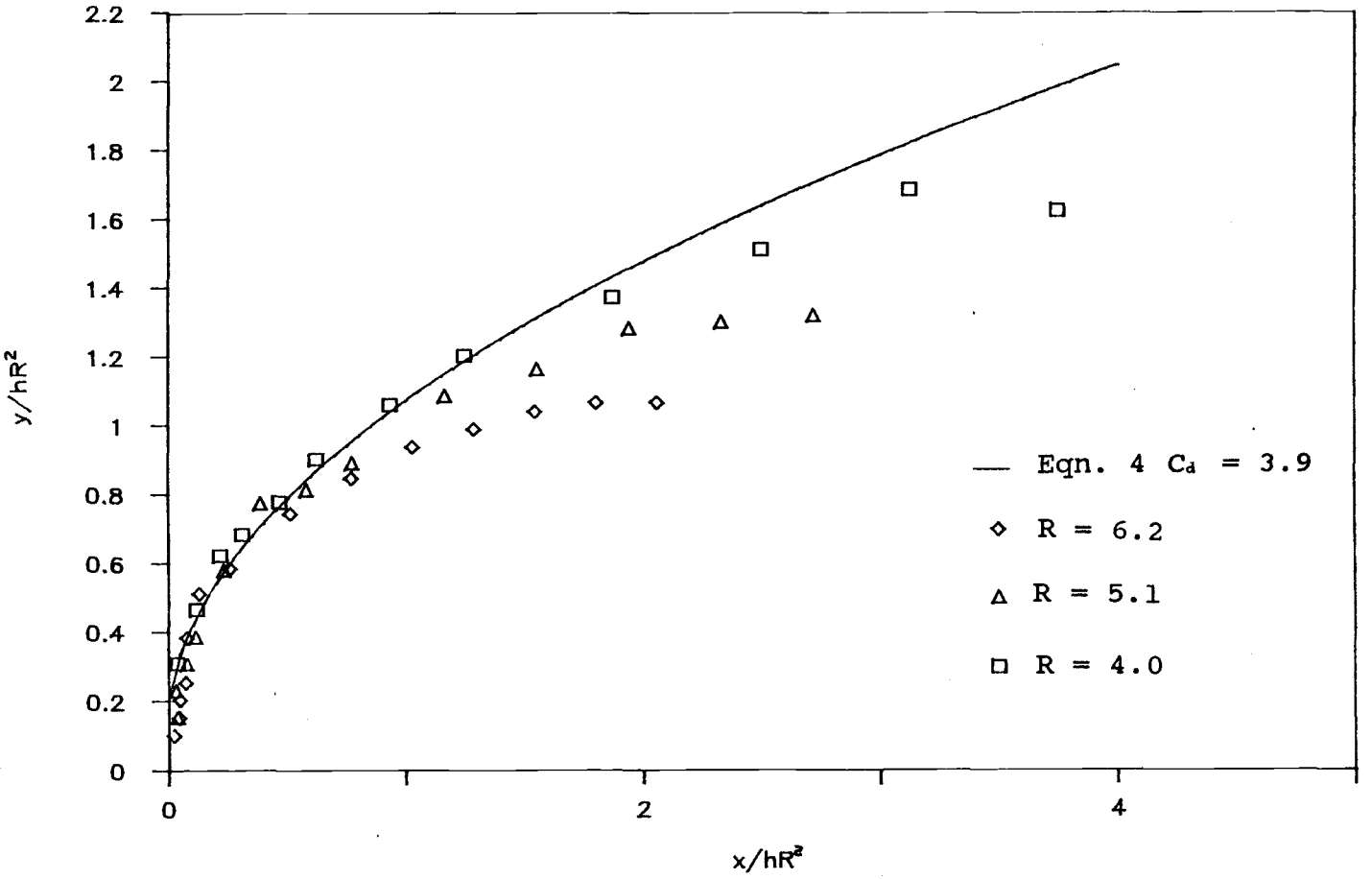

Figure 4.5. Jet axes reduces by R^2 for $\Theta = 75^\circ$

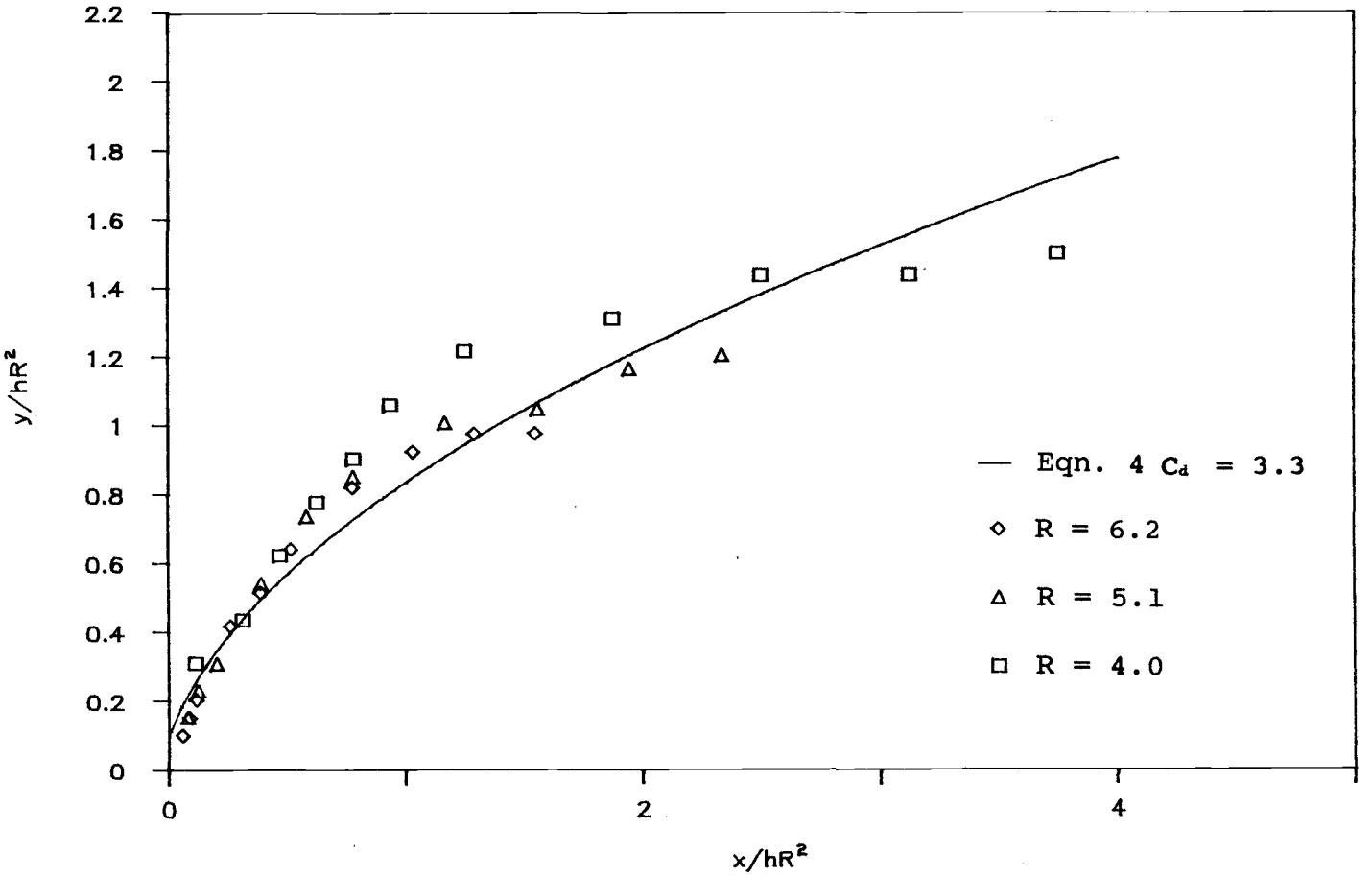

Figure 4.6. Jet axes reduced by R^2 for $\Theta = 60°$

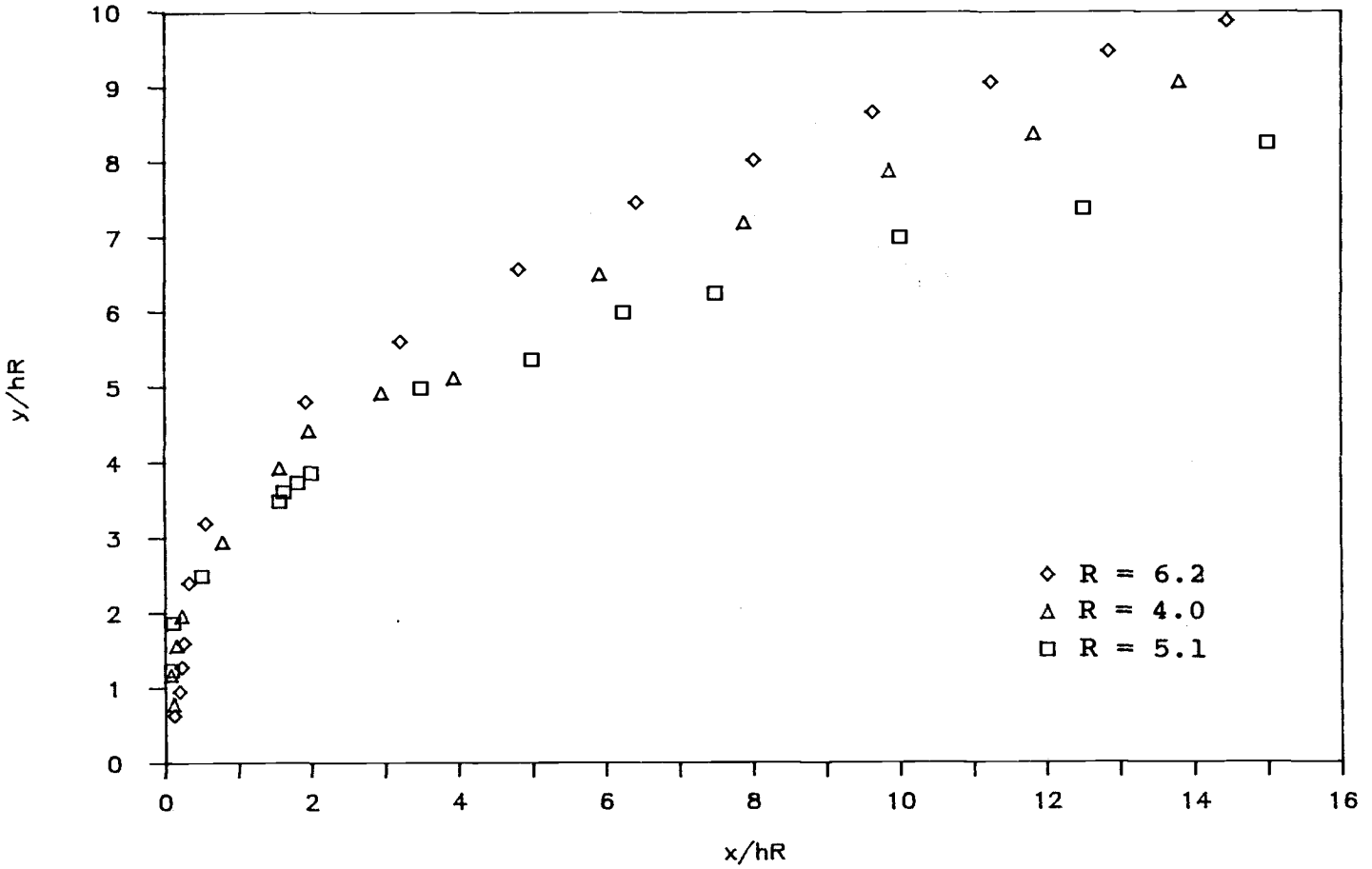

Figure 4.7. Jet axes reduced by R for $\theta = 90°$

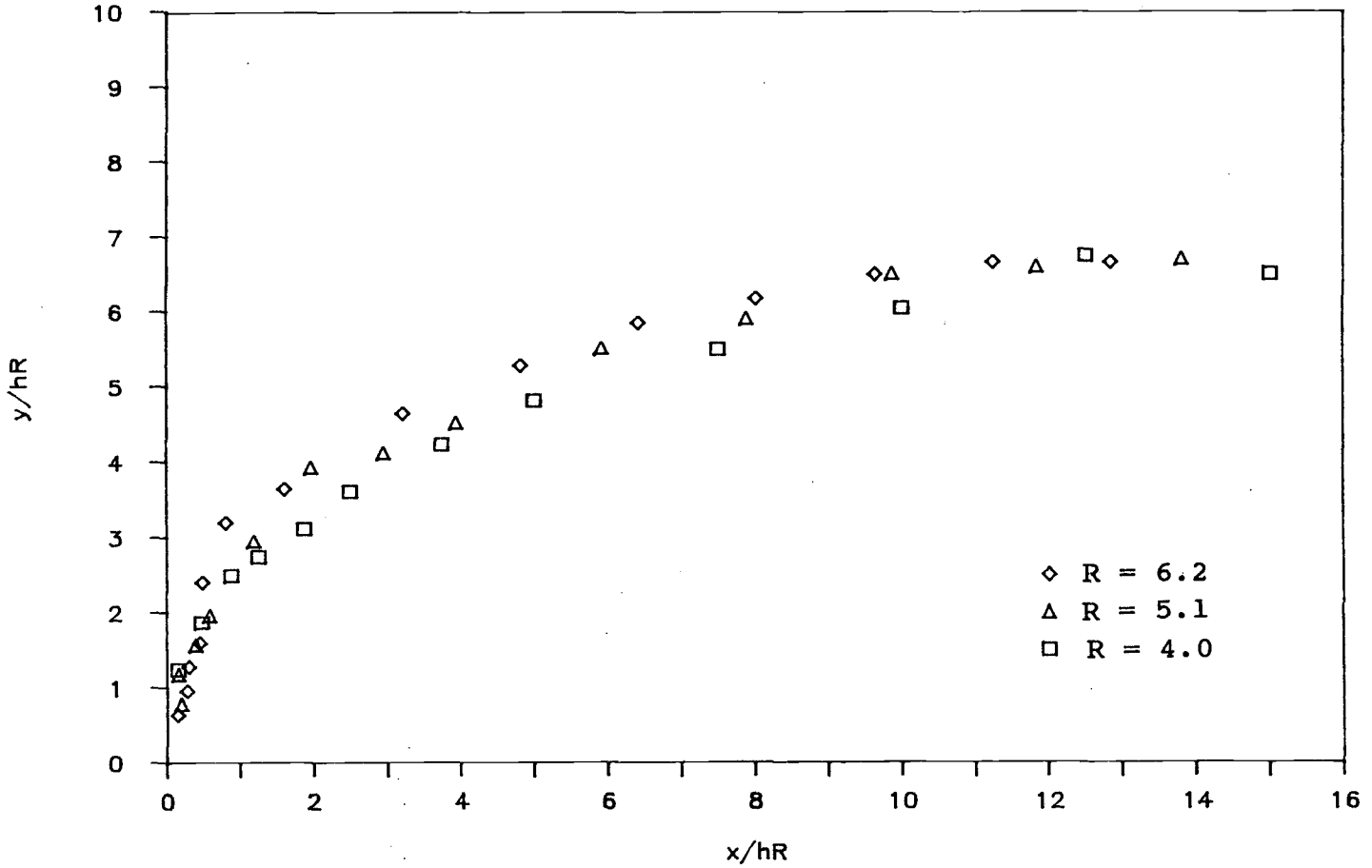

Figure 4.8. Jet axes reduced by R for $\Theta = 75^{\circ}$

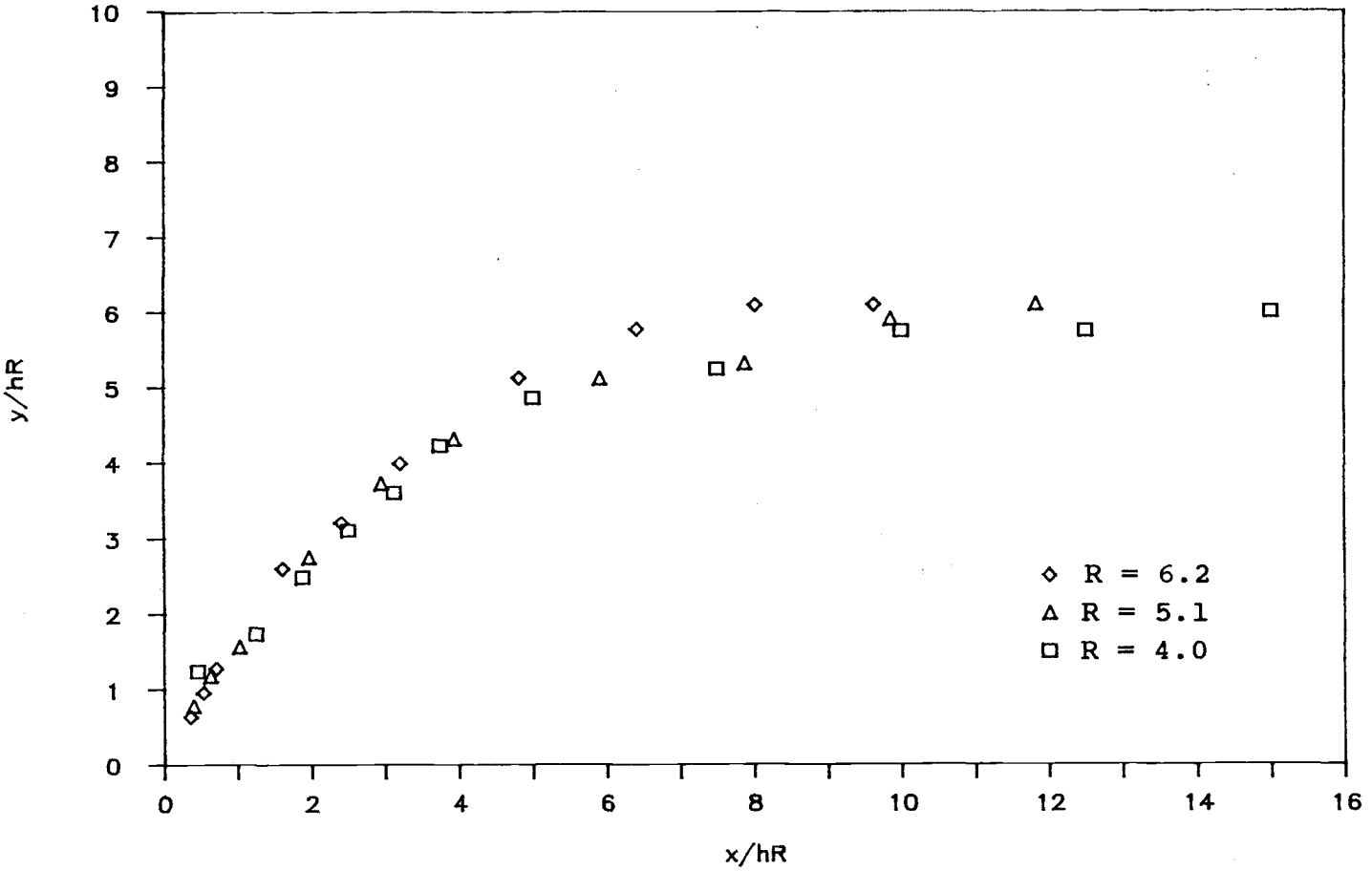

Figure 4.9. Jet axes reduced by R for $\theta = 60°$

not present a solid airfoil boundary to the mean flow as is assumed, but rather a fluid boundary where turbulent mixing occurs, where a higher drag coefficient is to be expected. In spite however of its departure from the data (its consistent indication of a higher slope of the jet axis at the downstream region, even for $\Theta = 90°$) the model can serve as a reasonable first approximation for the jet axis deflection, particularly for the normal jet, and can be useful because of its simplicity.

In response to the indication of a correlation of a power of R less than 2, the spatial non-dimensional coordinates were divided by R and the jet axes were plotted on the resulting coordinates (Figs. 4.7, 4.8, and 4.9). This type of correlation had been used for round jets in cross-flow to describe the far downstream region of the flow (Pratte and Baines 1967). As expected, the correlation for $\Theta = 90$ deg. was, in this case, not very good, under-compensating by not reducing the spatial scales enough. The division by R worked substantially better for $\Theta = 75$, and, particularly, 60 deg. indicating that the momentum effect plays a substantial role for the smaller angles of injection.

Once the jet axes trajectories were known the natural coordinate system of the jet: s (the jet axis) and n (direction normal to the jet axis) could be used to determine distances from the jet orifice, and the decay of excess axial velocity (Vc-Vm/Vj-Vm) could be determined.

Plots of the decay of axial velocity (Vc) with distance on jet axis (s/h) can be found in the appendix (Figs. A.1, A.2, and A.3). Distances along the s axis were measured by taking chord lengths on the plotted jet axes. A very good correlation of the decay of the excess axial velocity for the three different velocity ratios was achieved when the spatial coordinate was reduced by division with R (Fig. 4.10). A determination of the nature of this correlation was achieved by plotting the natural logarithms of the reduced spatial coordinate versus the excess axial velocity (Fig. 4.11). The decay of excess axial velocity was thus determined to be approximately linear in proportion to the -0.77 power of the s/hR coordinate.

It was not possible to determine the self-preservation properties of the flow because it was impossible to correlate the velocity profiles obtained.

The concept of similarity is that non-dimensional excess velocity profiles at a certain distance in the jet (a certain value of s/h) will be similar to profiles at any s/h and, by the use of an appropriate length scale, it will be possible to reduce all excess velocity profiles to one common curve. Similarity, inherently involves the natural axes of the jet and presumes that the velocity profiles are taken along the n axis. Determination, however of velocities along the normal to the jet axis (n axis) is complicated because it can only be based on the premise that the trajectory of the jet axis is known. In the case

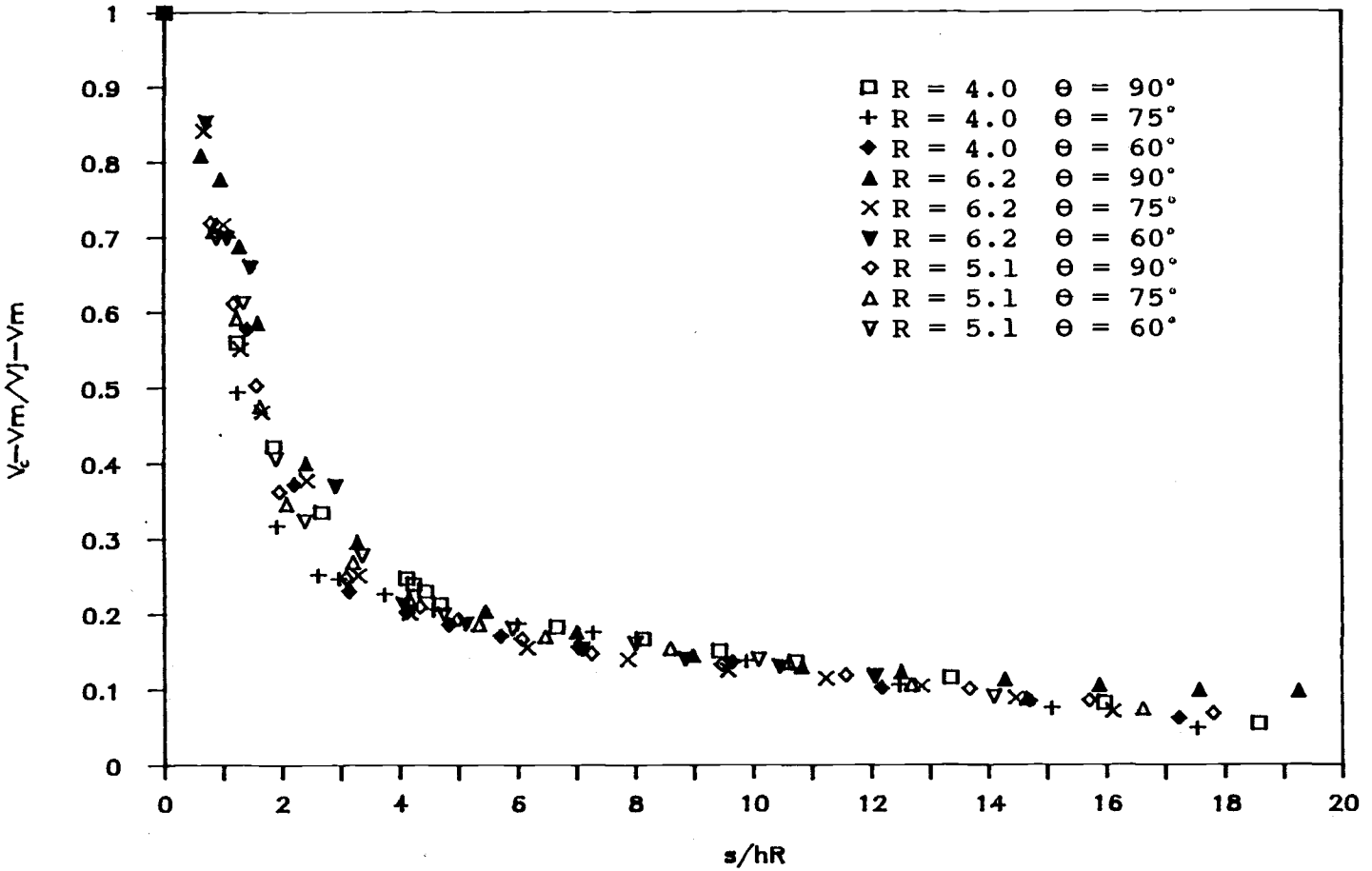

Figure 4.10. Decay of non-dimensional excess axial velocity

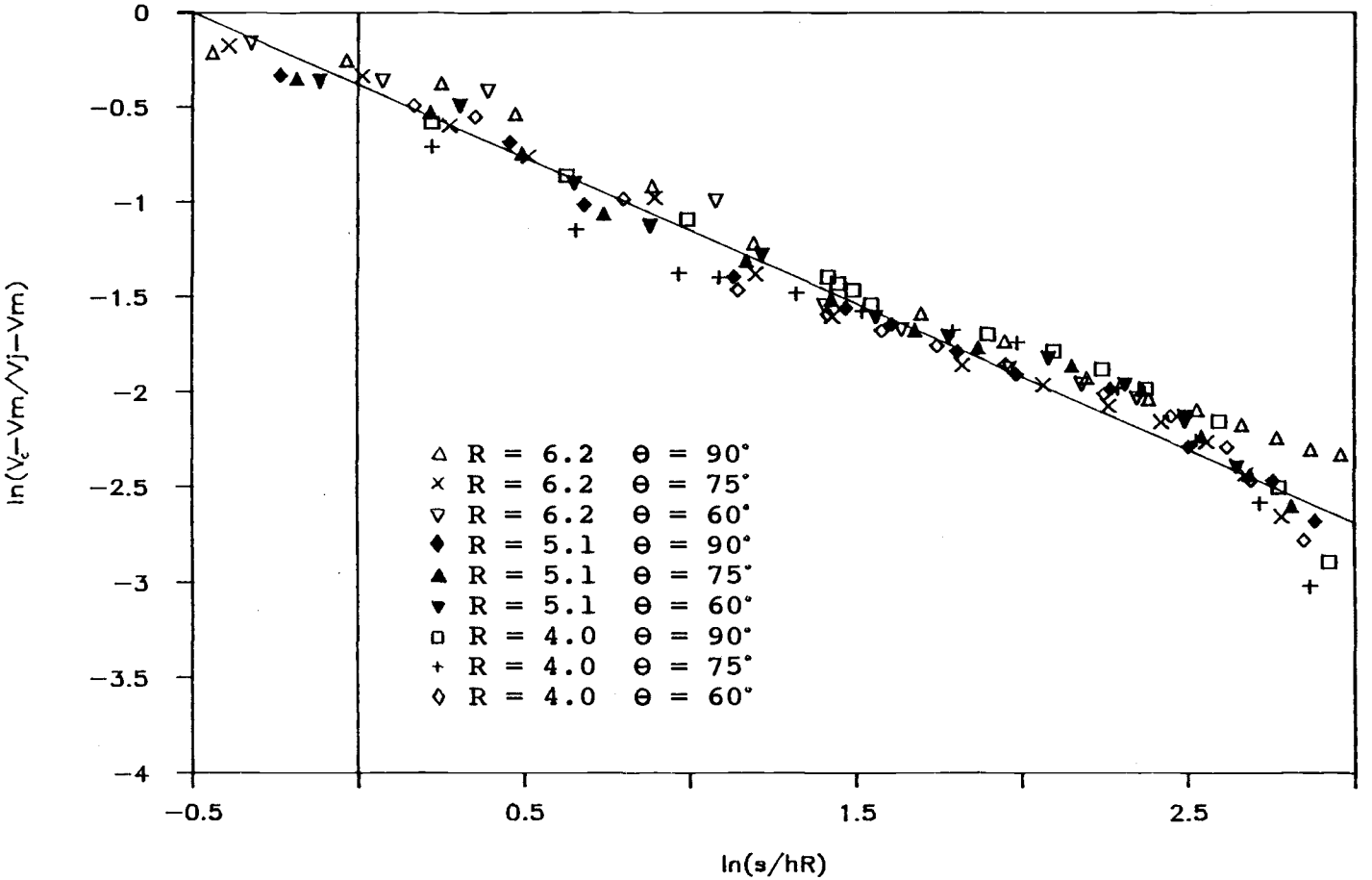

Figure 4.11. Logarithmic plot of the decay of non-dimensional excess axial velocity

that the trajectory is not known, it would have to be determined experimentally before traverses of the n direction could be done in order to determine the velocity profiles. Such a procedure would entail either performing dual sets of experiments (with conditions that are in most cases difficult to reproduce) or the capability of on-location data analysis.

A simpler way to approach the problem would be to try to obtain velocity profiles in regions of the jet flow where the angle of departure of the n axis from either the x or y direction is small, making an approximation of n by either x or y reasonable. Unfortunately, for an investigation (such as this) involving large angles of jet-to-cross-flow direction, such regions are either very small or very large distances from the jet orifice, where the experimental uncertainty (spatial resolution for the former and velocity resolution for the latter) is the greatest.

An attempt was made to correlate the velocity profiles obtained by x and y traverses by normalizing the velocities with the axis velocity for the particular traverse, and the length scales by the 50% velocity jet width (ie. distance from the axis where the excess non-dimensional velocity reached the value 0.5). This correlation was not good, showing considerable scatter that could be traced back to either significant deviation from the n direction or inherently large experimental error (Fig. 4.12, graphs of the individual velocity profiles can be found in the

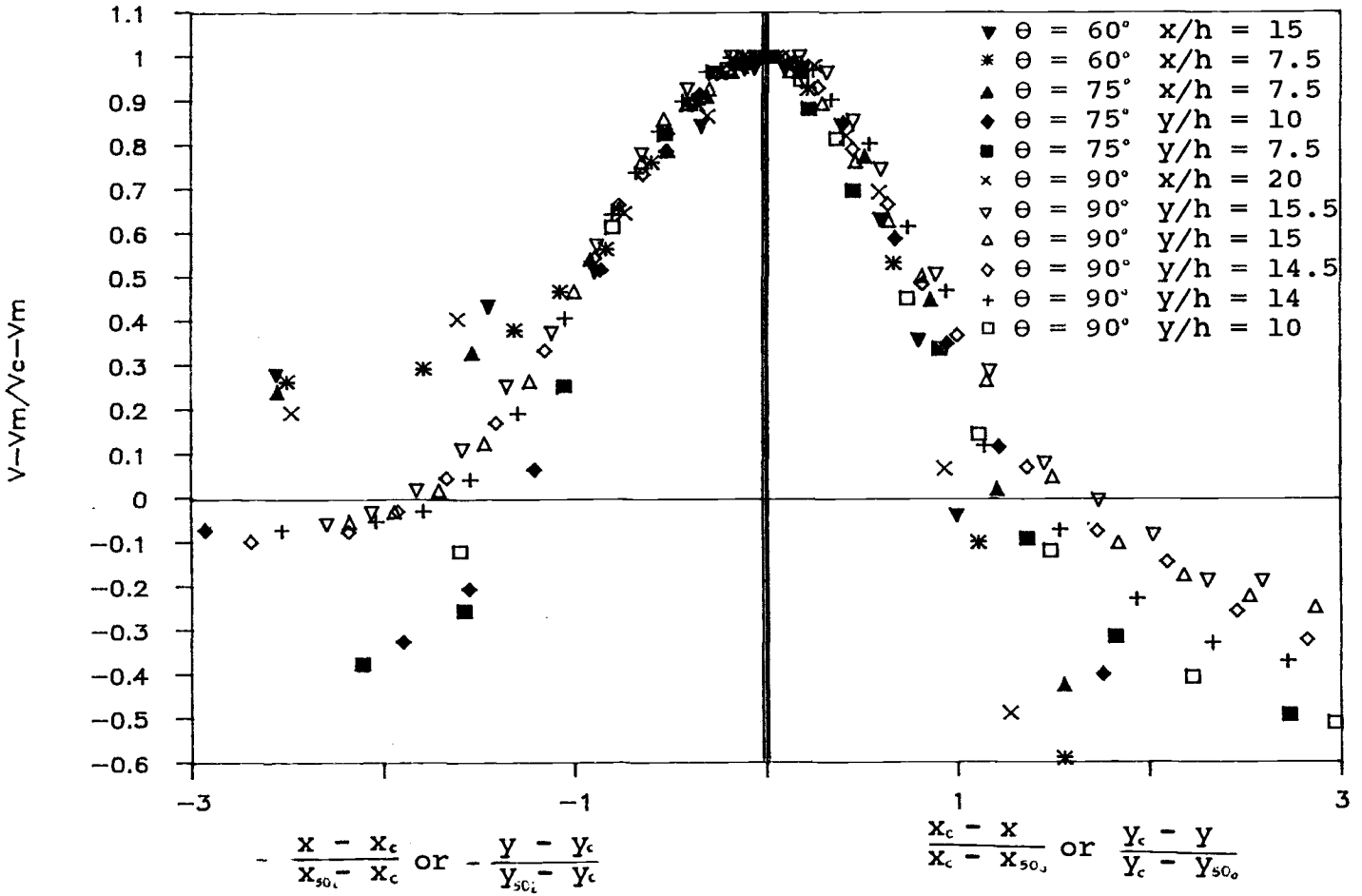

Figure 4.12. Normalized velocity distribution in jet cross-section for R

appendix) and no conclusions on velocity profile similarity can be drawn from it. The possibility to use the experimentally determined jet axes and axial velocity correlation in order to refer each velocity datum to its particular axis velocity and n location was examined but was not chosen because it involved individual treatment of each datum that would invalidate any attempted correlation even if the large uncertainties inherent in such a process were not taken into consideration.

5. CONCLUSIONS

The purpose of this investigation was to determine the momentum diffusion characteristics of plane jets in a cross-flow in order to provide some background so that a prediction can be made as to whether the preswirl concept for the Volumetric Air Heating Receiver would be feasible. The conclusions that can be drawn from the correlations of the experimental data are: 1) The jet trajectories can be reasonably predicted independently of the value of the jet-to-cross-flow velocity ratio R if the appropriate correlation (either of R^2, or R) is used. 2) The non-dimensional excess velocity decay can be well predicted as a linear function of the -0.77 power of the non-dimensional natural length scale s/h reduced by R (Eqn. 5).

$$Vc-Vm/Vj-Vm = (s/hR)^{-.77} \qquad [5]$$

3) There can be no conclusion drawn about the similarity of velocity profiles from the data taken.

Conclusions 1) and 2) are, in effect, enough to make a reasonable prediction about the feasibility of the preswirl concept for the V.A.H.R., namely, that it appears that for a large enough velocity ratio, R, and jet orifice aperture, h, the plane jets will penetrate into the cross-flow at a great enough distance, and with a high enough excess velocity to

make only a small number of slot jets necessary (4 to 8). The main design consideration would then be whether a large enough flow rate would be feasible to produce. It should be noted however that the interference of the flowfields of the circumferentially arranged jets might significately effect the overall flow situation, possibly in a positive way: the jet flows by interfering with one another might very well strengthen the penetration characteristics of each other thus lowering the necessary values of R and h and, consequently, requiring smaller air flow rates. In order to determine with a better degree of ceratinty the flow characteristics of the preswirl V.A.H.R., it is suggested that a scaled model of the receiver be constructed and tested.

REFERENCES

Abramovich, G. N., 1963. The Theory of Turbulent Jets, MIT Press, Cambridge, Massachusetts.

Andreopoulos, J., 1981. "Comparison Test of the Response to Pitch Angles of Some Hot Wire Anemometry Techniques." Rev. Sci. Instrum. Vol. 52(9). pp. 1376-1381.

Bird, S. P. et al. 1982. "Evaluation of Solar Air Heating Central Receiver Concepts." PNL-4003, Pacific Northwest Laboratory Richland, Washington.

Birkhoff, G. & Zarantonello, E. H., 1957. Jets, Wakes, and Cavities, Academic Press Inc., New York, New York.

Bradbury, L. J. S., 1965. "The Structure of a Self-Preserving Turbulent Plane Jet." J. Fluid Mech. Vol. 23, pp. 31-64.

Browne, L. W. B., Antonia, R. A. & Chambers, A. J., 1984. "The Interaction Region of a Turbulent Plane Jet." J. Fluid Mech. Vol. 149. pp. 355-373.

Choi, Y. & Wood, I. R., 1966. "Momentum Diffusion From a Two-Dimensional Jet." Water Research Laboratory, Univ. of New South Wales, Australia, Report 90.

Crabb, D., Durao, D. F. G., & Whitelaw, J. H., 1981. "A Round Jet Normal to a Crossflow." J. Fluids Eng. Vol. 103. pp. 142-153.

DeLaquil, P., III, Young, C. L., & Noring, J. E., 1983. "Solar Central Receiver High Temperature Process Air Systems." SAND82-8254, Sandia National Laboratories, Livermore, California.

Drost, M. K., 1985. "Volumetric Receiver Development - A Heat Transfer and Design Evaluation of an Advanced Air Heating Solar Thermal Central Receiver Concept." Ph.D. Thesis, Oregon State University, Corvallis, Oregon.

Drost M. K. & Eyler, L. L., 1981. "Preliminary Evaluation of the Volumetric Air Heating Receiver." Paper No. 81-WA/Sol-26, American Society of Mechanical Engineers Winter Annual Meeting.

Everitt, K. W. & Robins, A. G., 1978. "The Development and Structure of Turbulent Plane Jets." J. Fluid Mech. Vol. 88, Part 3. pp. 563-583.

Friehe, C. A. & Schwarz, W. H., 1968. "Deviations From the Cosine Law for Yawed Cylindrical Anemometer Sensors." J. Appl. Mech. Vol. 35E. pp. 655-662.

Girshovich, T. A., 1966 a. "The Turbulent Jet in a Cross Flow." Fluid Mechanics, Vol. 1, No. 1. pp. 108-109.

Girshovich, T. A., 1966 b. "Theoretical and Experimental Study of a Plane Turbulent Jet in a Cross Flow." Fluid Mechanics, Vol. 1, No. 5, pp. 84-87.

Keffer, J. F. & Baines, W. D., 1963. "The Round Turbulent Jet in a Cross-Wind." J. Fluid Mech., Vol. 15, pp. 481-496.

Moussa, Z. M., Trischka, J. W., & Eskinazi, S., 1977. "The Near Field in the Mixing of a Round Jet with a Cross Stream." J. Fluid Mech., Vol. 80, Part 1, pp. 49-80.

Platten, J. L. & Keffer, J. F., 1971. "Deflected Turbulent Jet Flows" Trans. A.S.M.E., J. Appl. Mech., pp. 756-758.

Pratte, B. D. & Baines, W. D., 1967. "Profiles of The Round Turbulent Jet in a Cross-Flow." Proc. A.S.C.E., J. Hydraul. Div., Vol 93, pp. 53-64.

Rajaratnam, N., 1976. Turbulent Jets, Elsevier Scientific Publishing Company, Amsterdam - Oxford - New York.

Ramparian, B. R. & Chandrasekhara, M. S., 1985. "LDA Measurements in Plane Turbulent Jets." J. Fluids Eng., Vol. 107.

Schetz, J. A., 1980. Injection and Mixing in Turbulent Flow, PROGRESS IN ASTRONAUTICS AND AERONAUTICS, Vol. 68, American Institute of Aeronautics and Astronautics, New York, New York.

Tutu, N. K. & Chevray, R., 1975. "Cross-Wire Anemometry in High Intensity Turbulence." J. Fluid Mech., Vol. 71, Part 4, pp. 785-800.

APPENDIX

APPENDIX

What follows are graphs of the experimental data obtained in this investigation. The graphs include the velocities at the jet axes, and the velocity profiles obtained at various locations in the jet for all nine experimental conditions. The velocity profiles are normalized excess velocities (V-Vm/Vc-Vm), but the axis and cross-flow velocities for each are given.

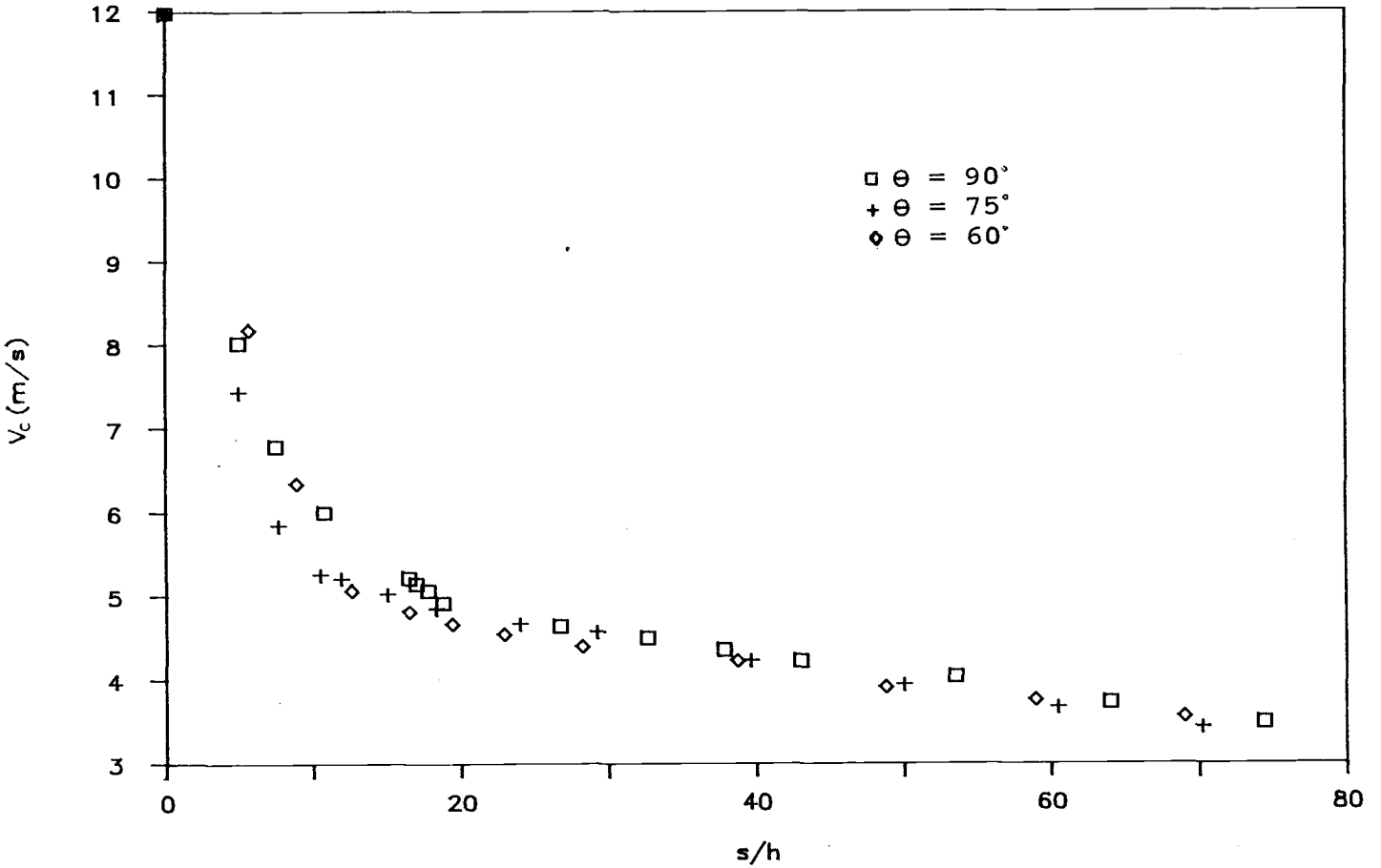

Figure A.1. Decay of axial velocity for R = 4.0

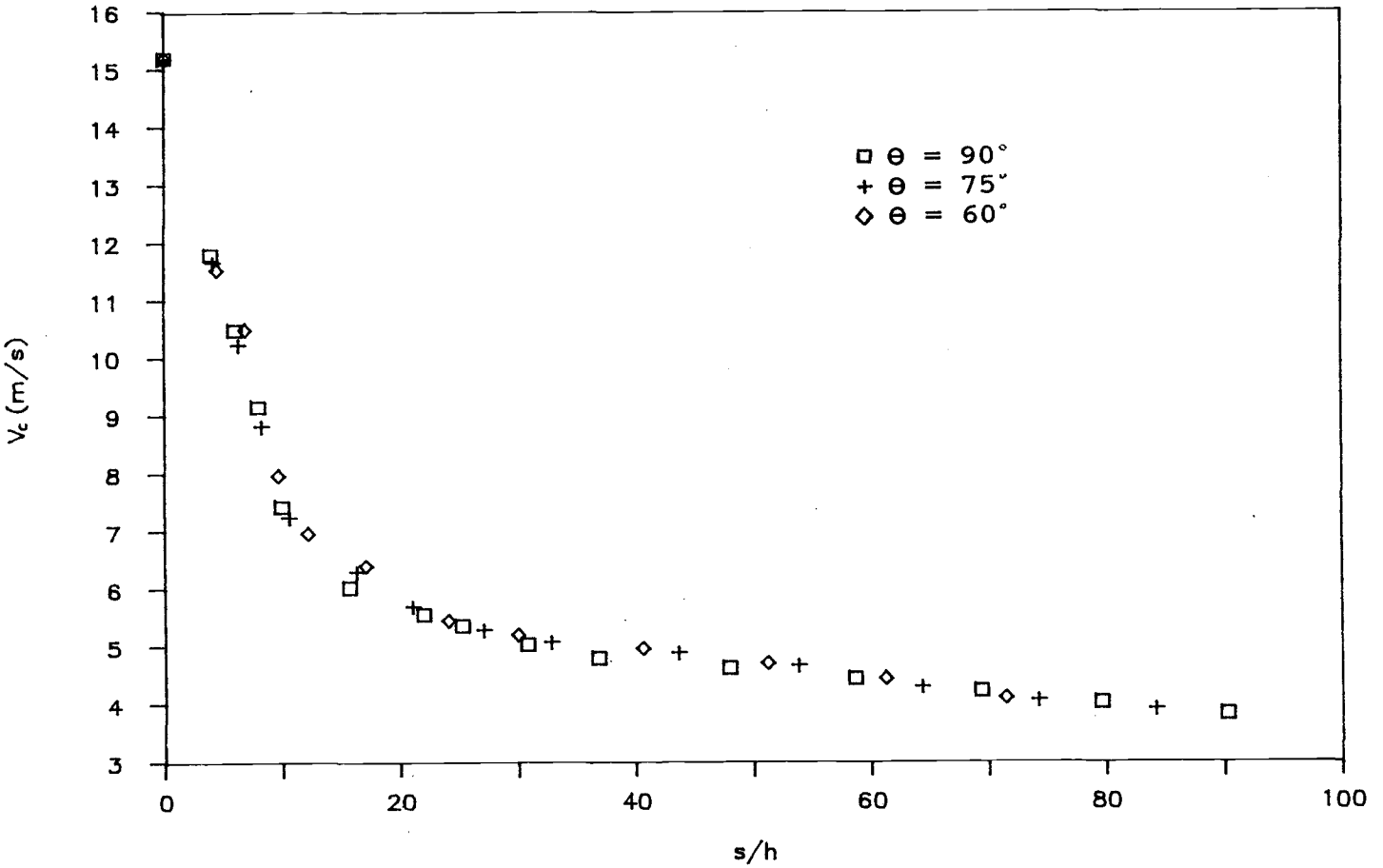

Figure A.2. Decay of axial velocity for R = 5.1

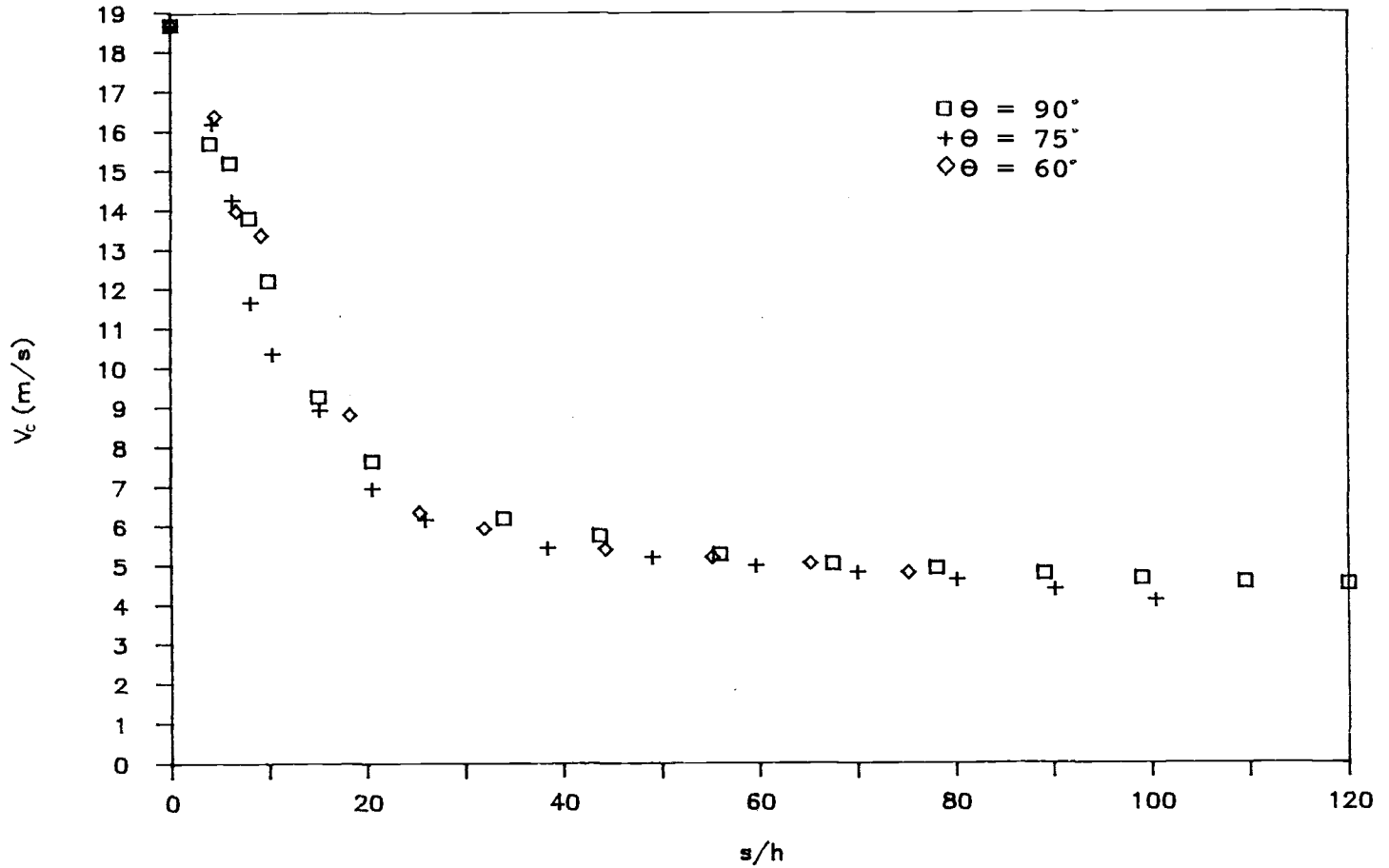

Figure A.3. Decay of axial velocity for R = 6.2

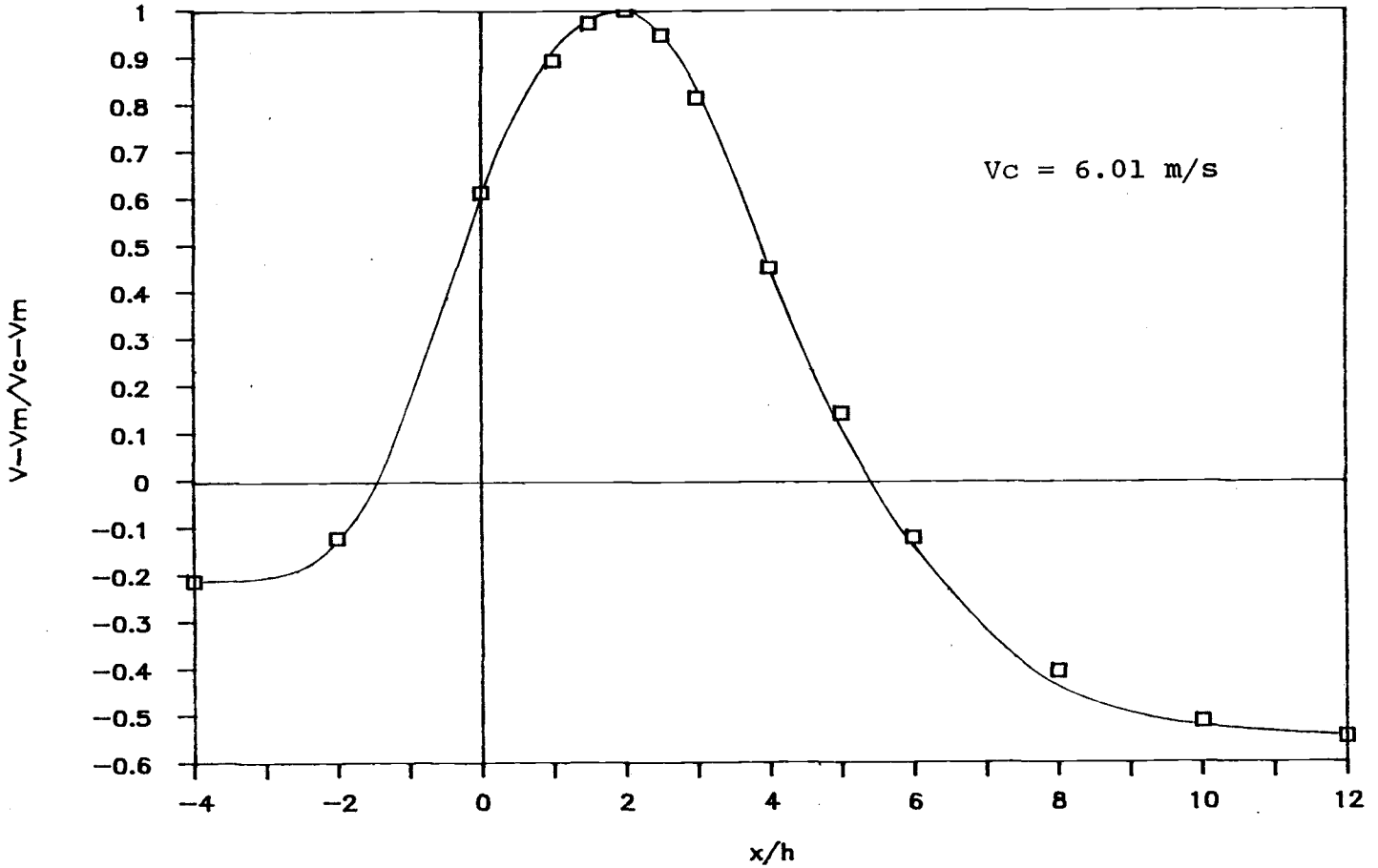

Figure A.4. Velocity distribution in jet cross section for R = 4.0, $\Theta = 90^{\circ}$, y/h = 10

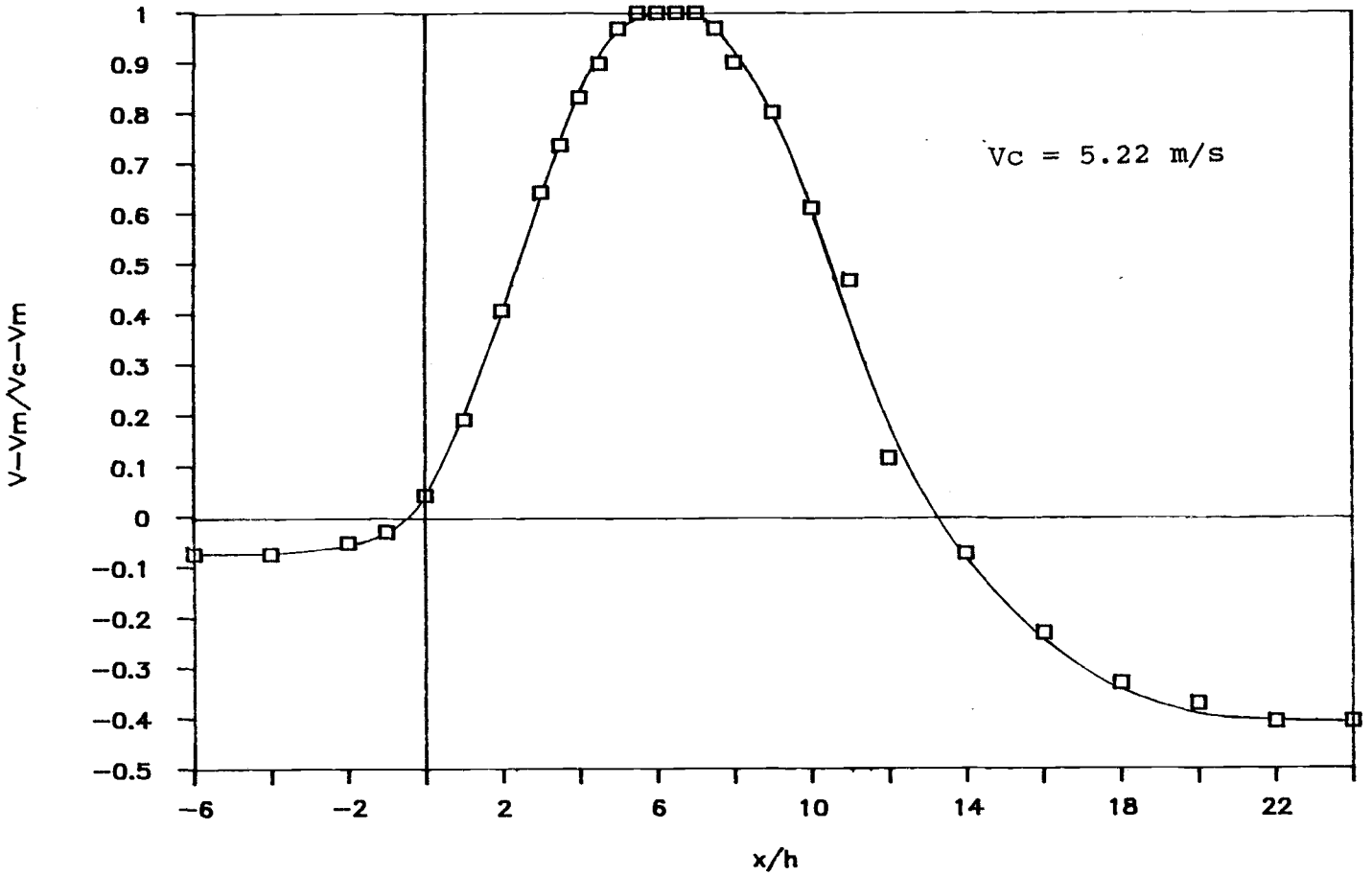

Figure A.5. Velocity distribution in jet cross section for R = 4.0, $\theta = 90^{\circ}$, y/h = 14

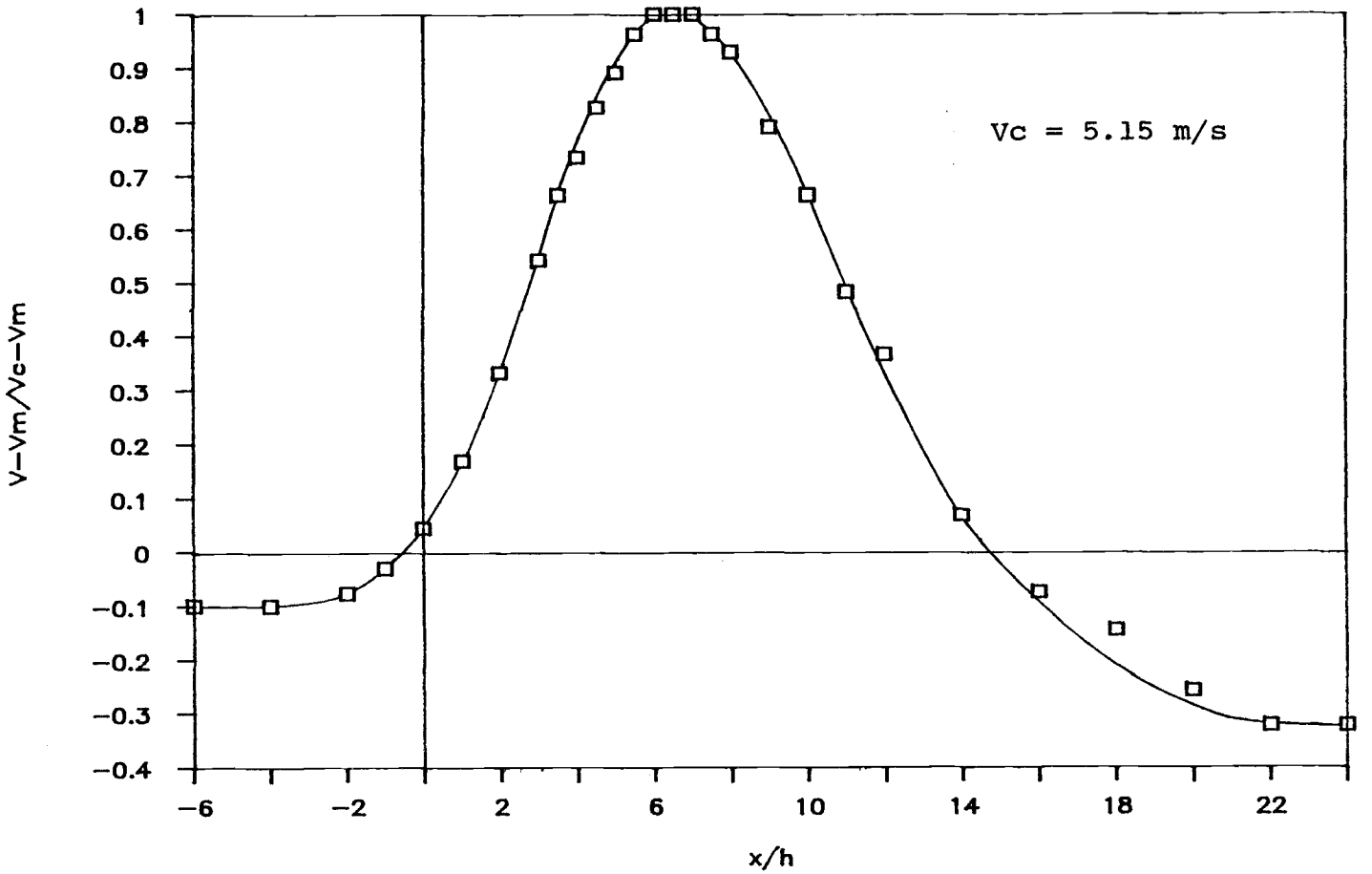

Figure A.6. Velocity distribution in jet cross section for R = 4.0, θ = 90°, y/h = 14.5

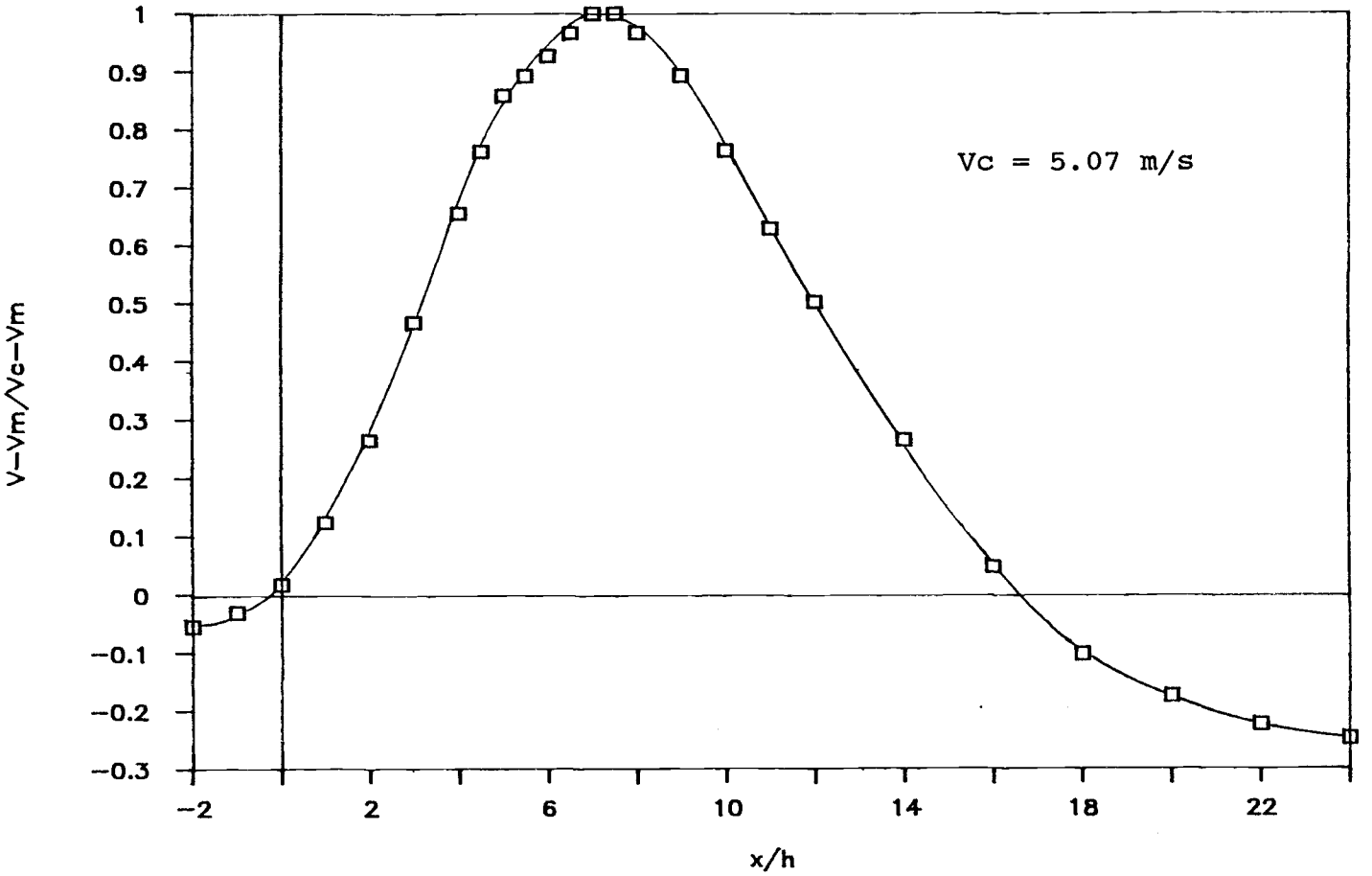

Figure A.7. Velocity distribution in jet cross section for R = 4.0, θ = 90°, y/h = 15

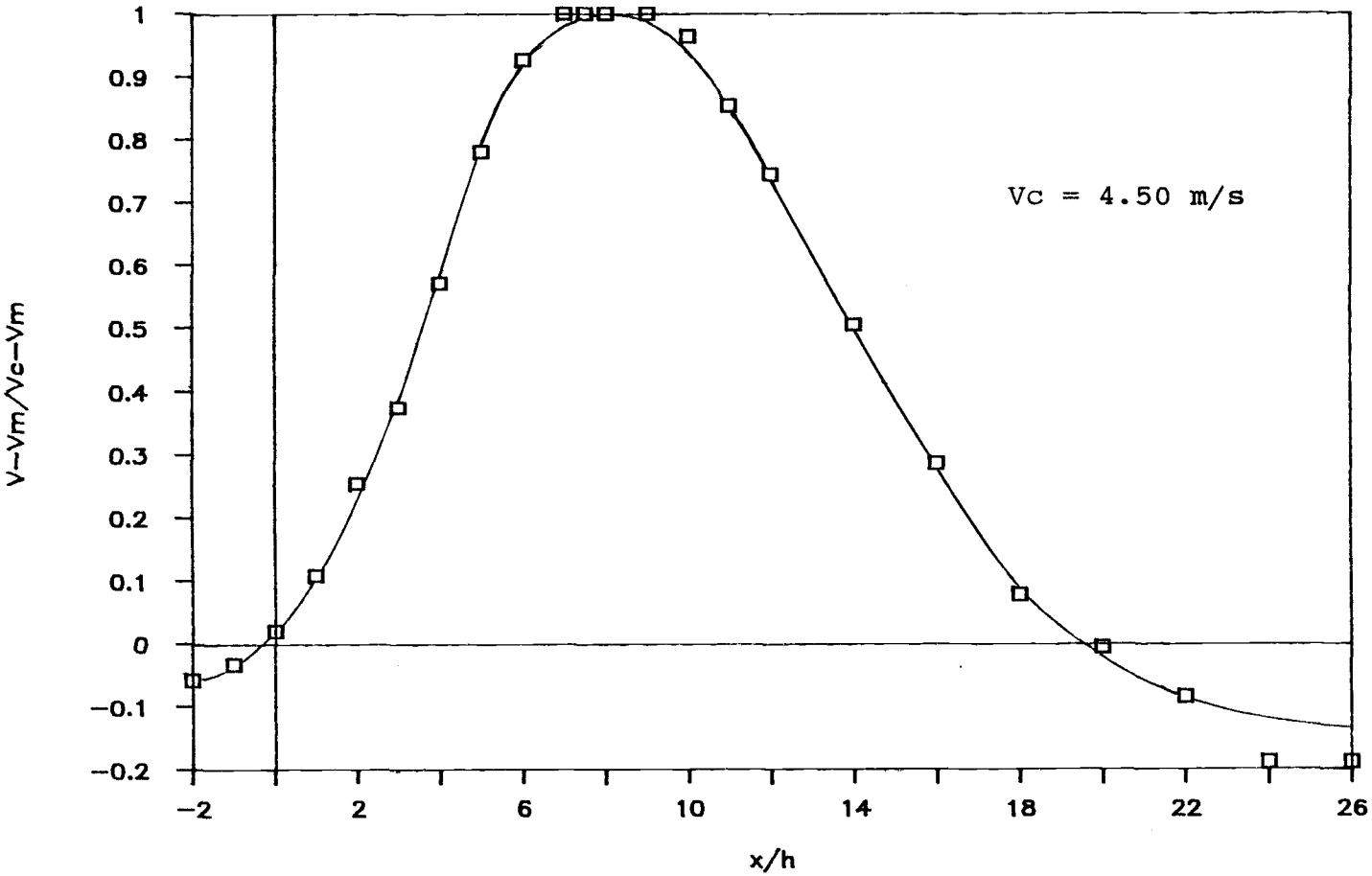

Figure A.8. Velocity distribution in jet cross section for R = 4.0, θ = 90°, y/h = 15.5

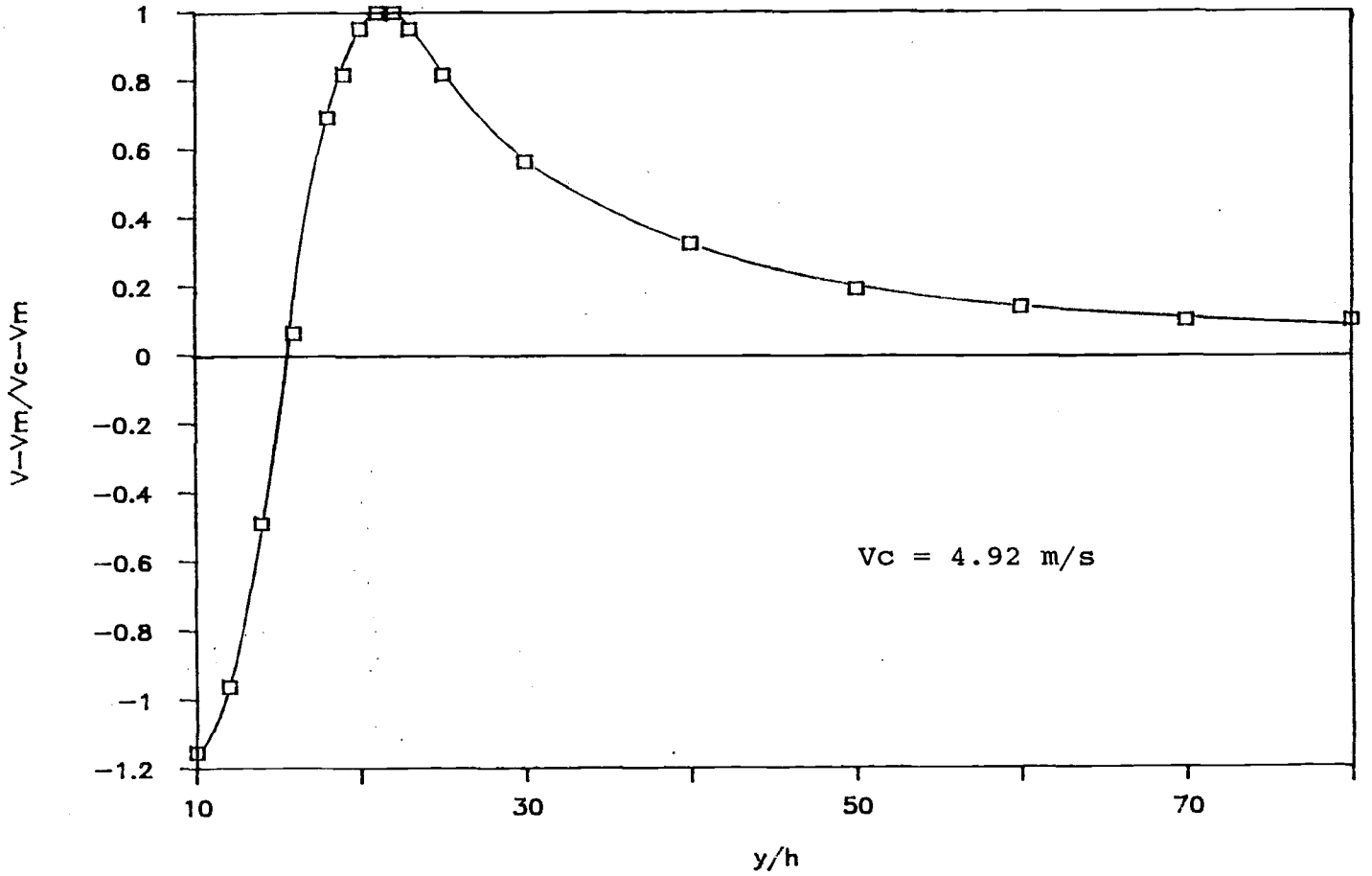

Figure A.9. Velocity distribution in jet cross section for R = 4.0, θ = 90°, x/h = 20

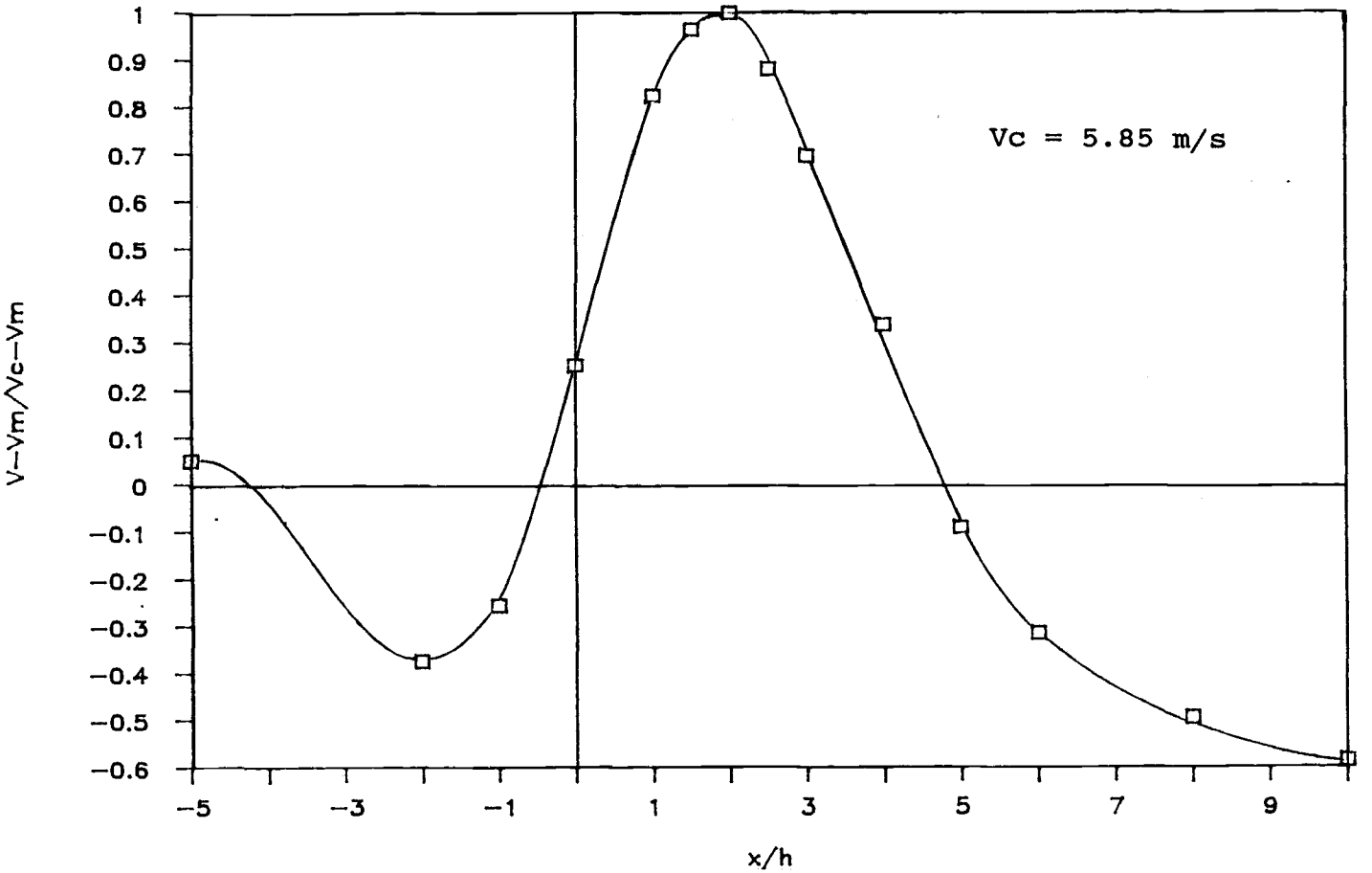

Figure A.10. Velocity distribution in jet cross section for R = 4.0, $\Theta = 75^{\circ}$, y/h = 7.5

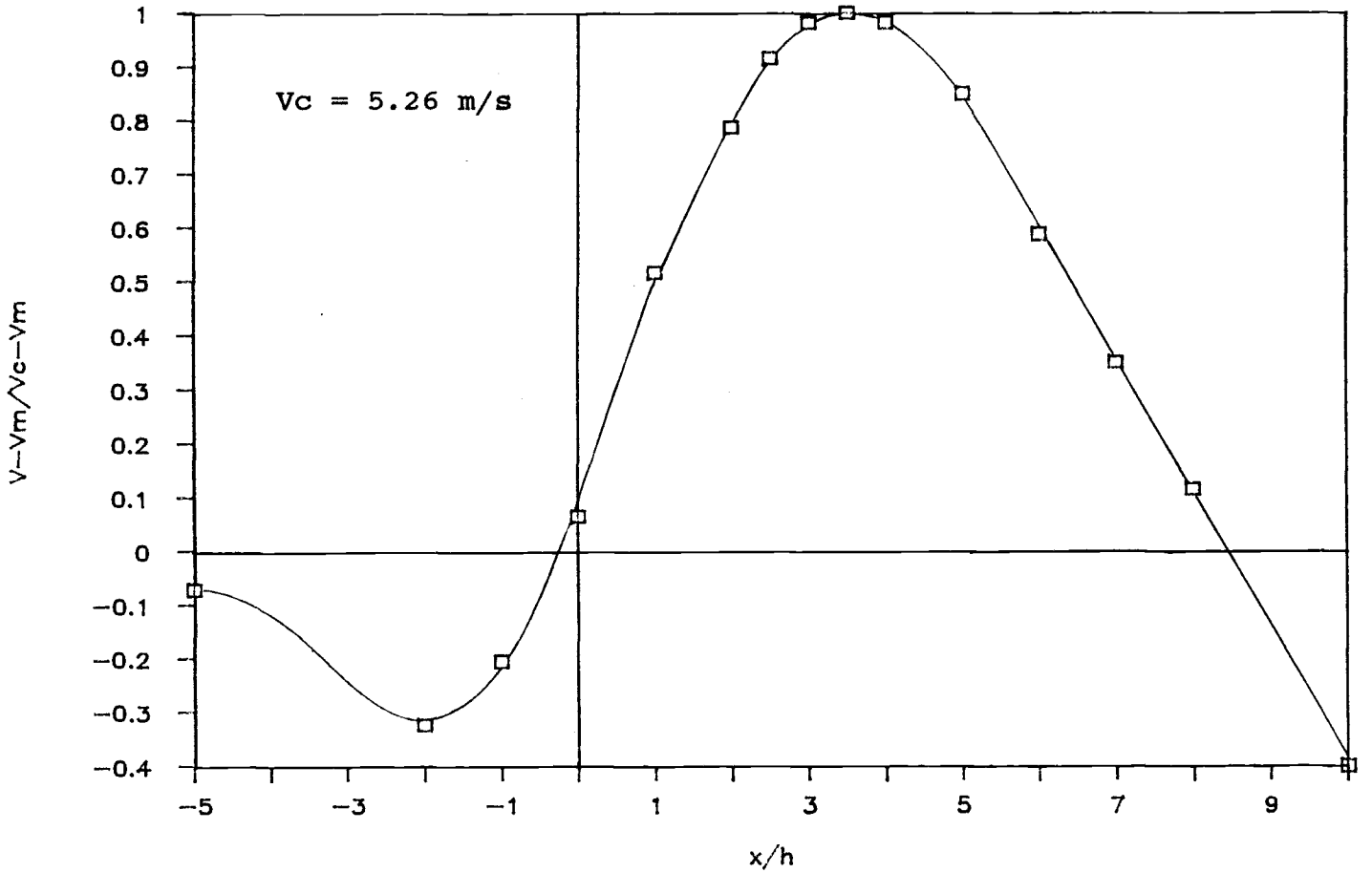

Figure A.11. Velocity distribution in jet cross section for R = 4.0, $\theta = 75^{\circ}$, y/h = 10

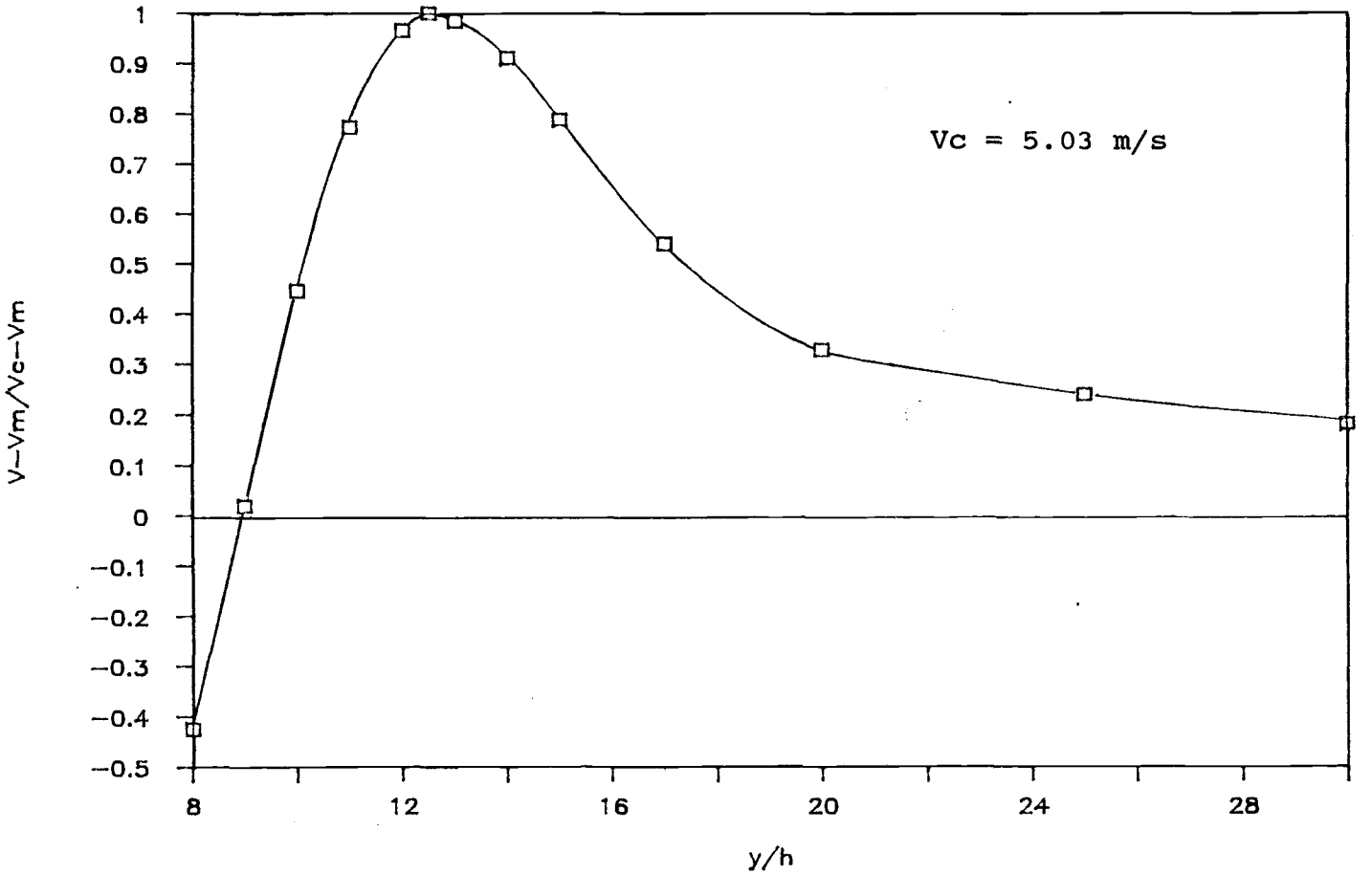

Figure A.12. Velocity distribution in jet cross section for R = 4.0, $\Theta = 75^{\circ}$, x/h = 7.5

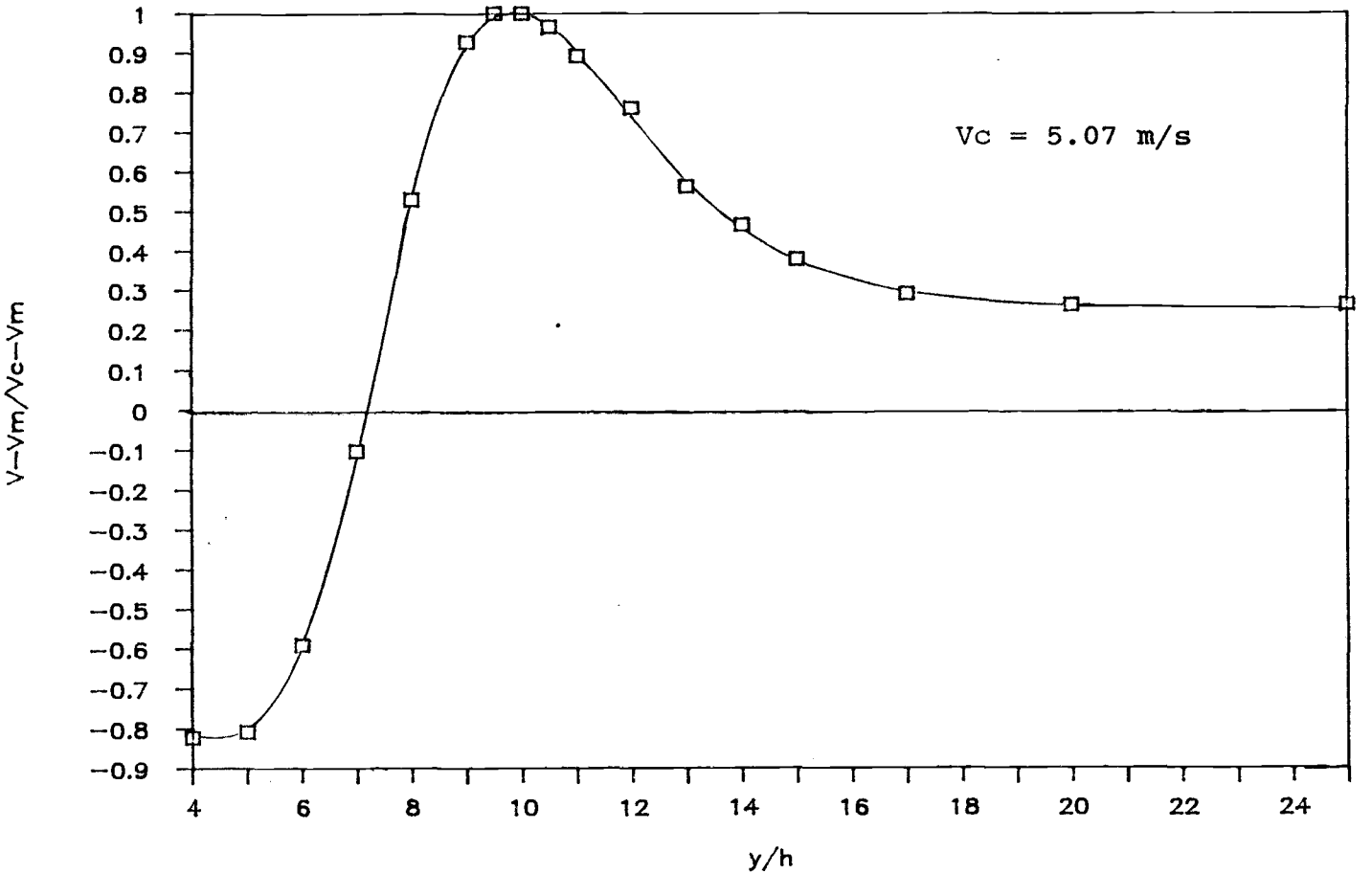

Figure A.13. Velocity distribution in jet cross section for R = 4.0, $\Theta = 60^{\circ}$, x/h = 7.5

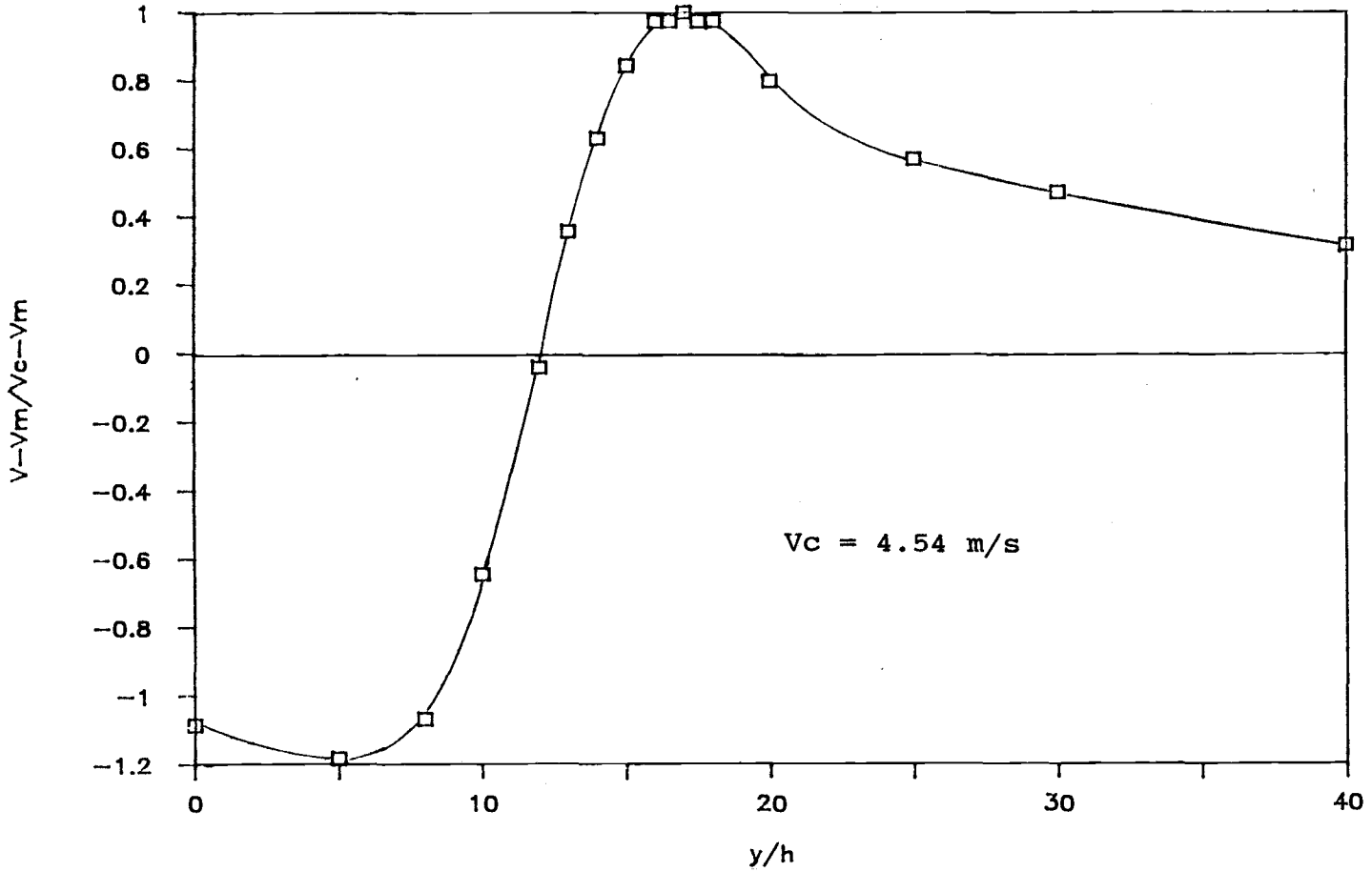

Figure A.14. Velocity distribution in jet cross section for R = 4.0, $\Theta = 60^{\circ}$, x/h = 15

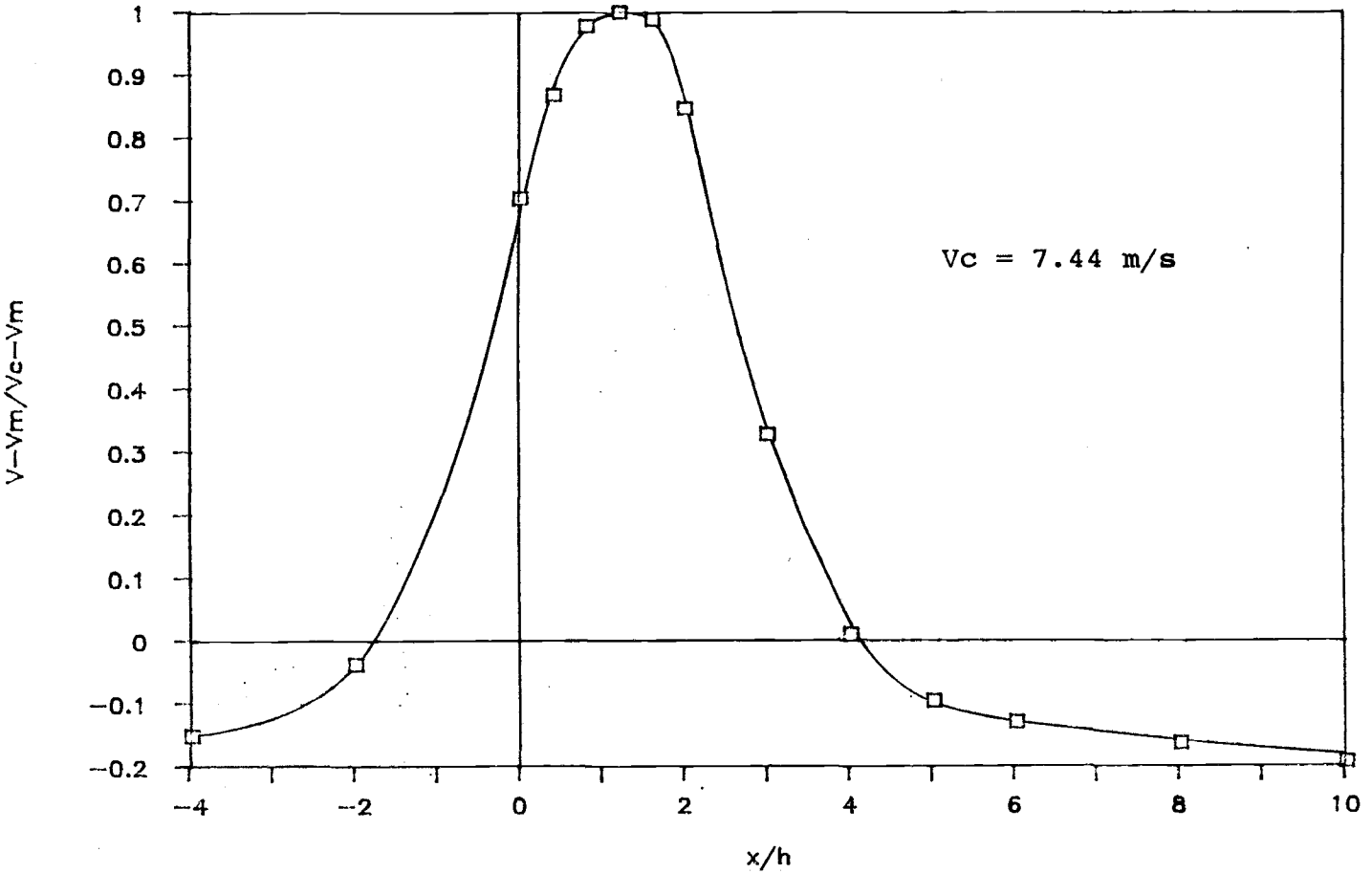

Figure A.15. Velocity distribution in jet cross section for R = 5.1, $\Theta = 90^{\circ}$, y/h = 10

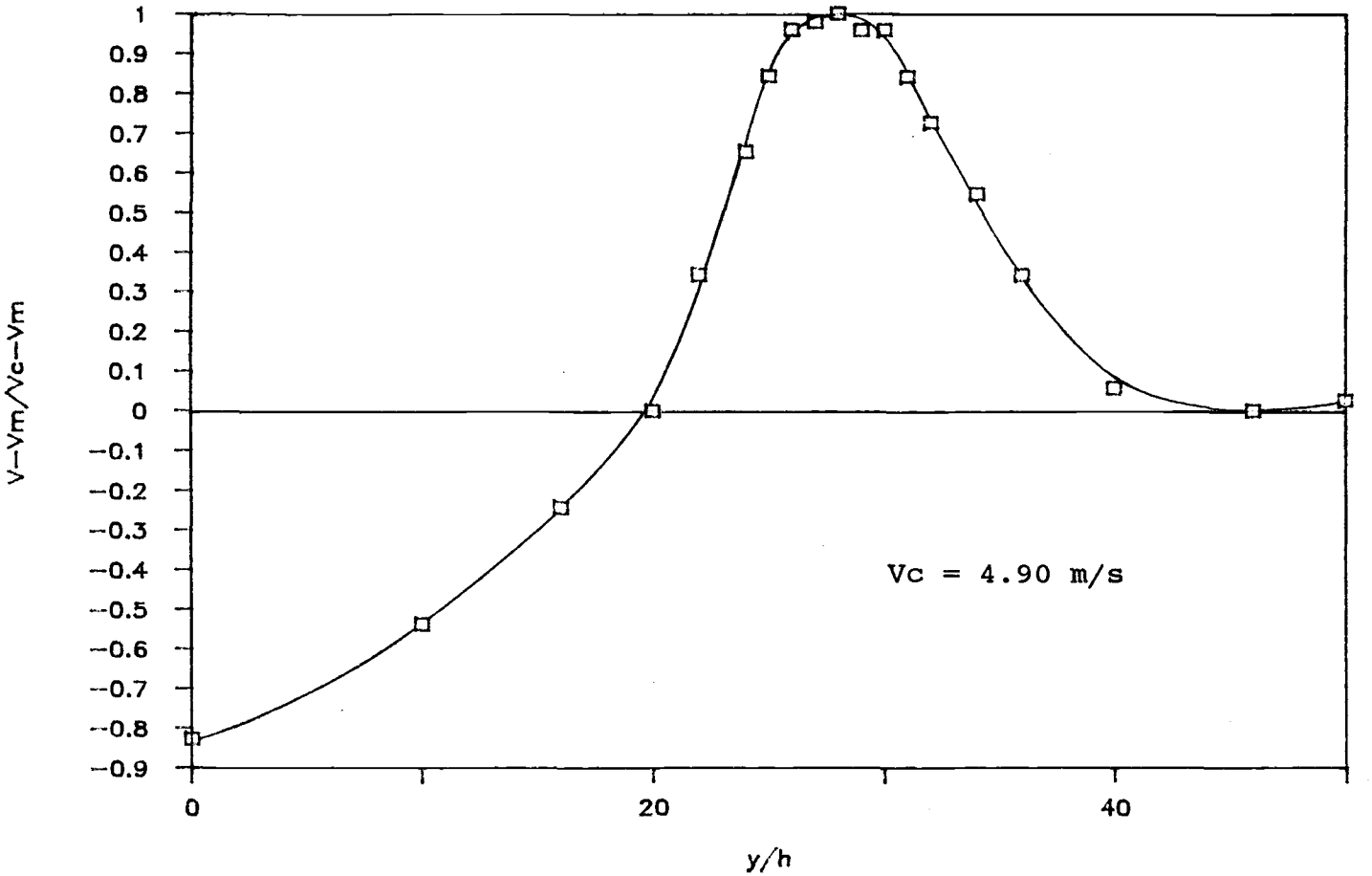

Figure A.16. Velocity distribution in jet cross section for R = 5.1, $\theta = 75^{\circ}$, x/h = 30

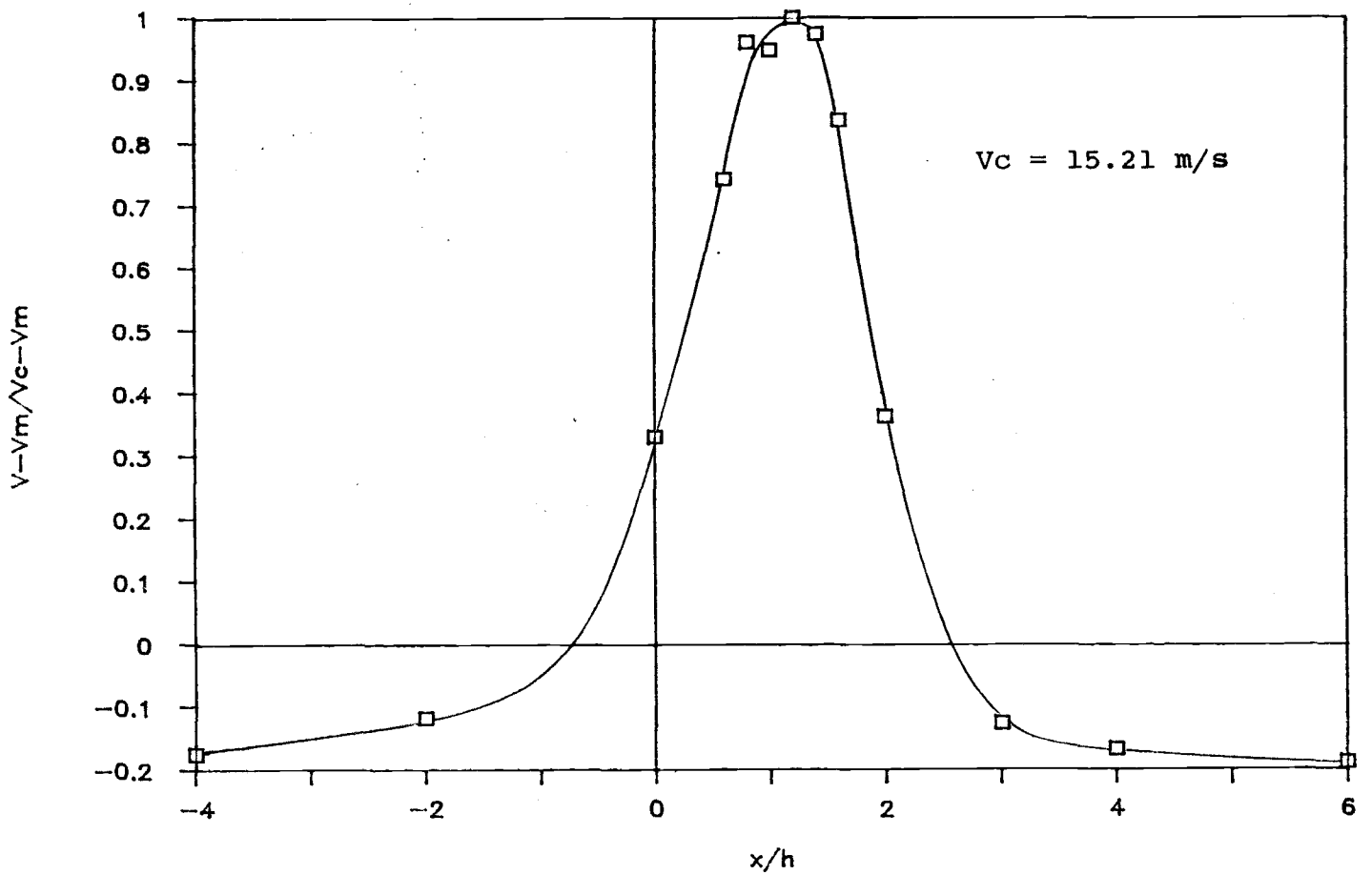

Figure A.17. Velocity distribution in jet cross section for R = 6.2, $\theta = 90^{\circ}$, y/h = 6

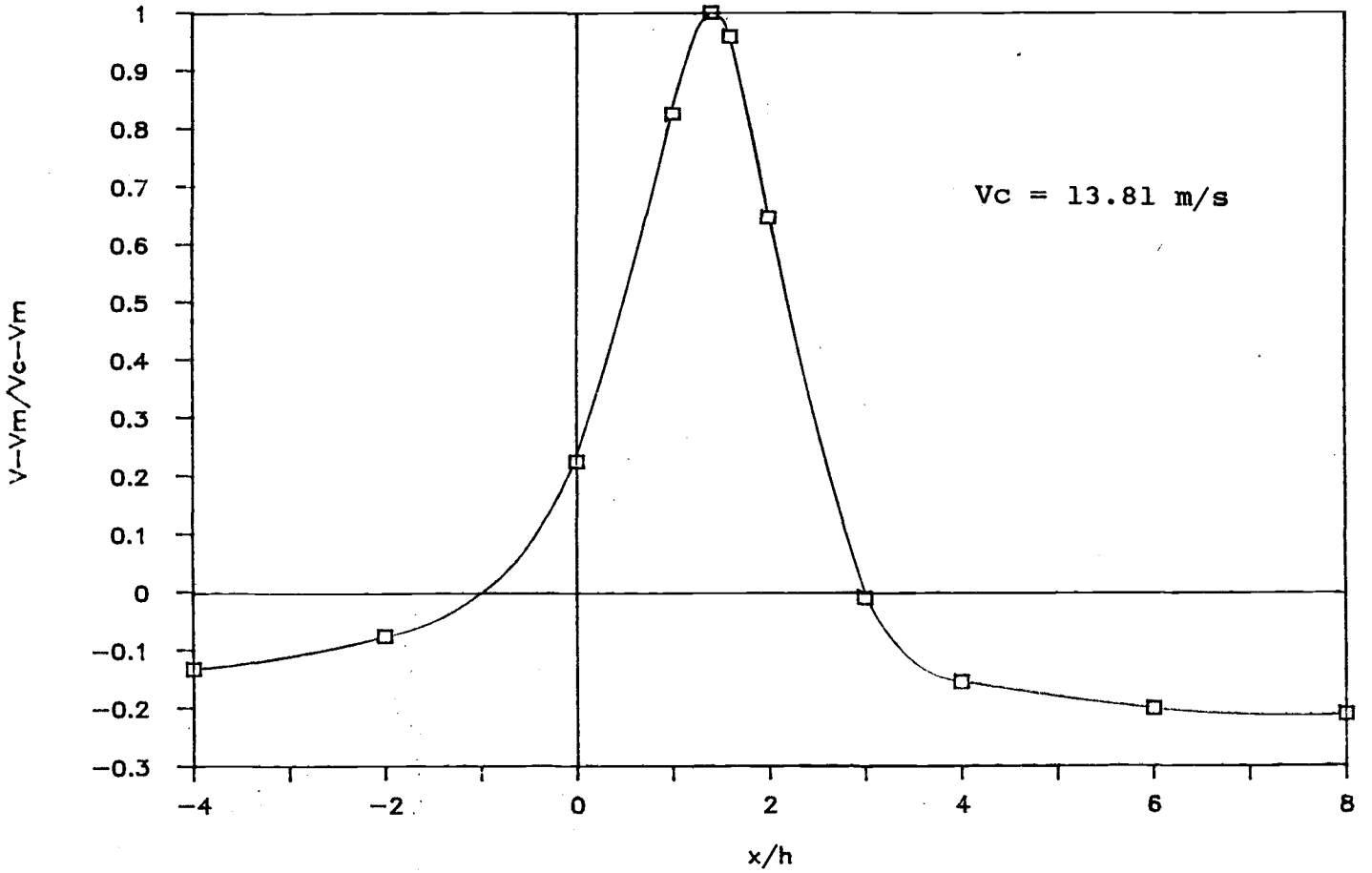

Figure A.18. Velocity distribution in jet cross-section for R = 6.2, $\Theta = 90^{\circ}$, y/h = 8

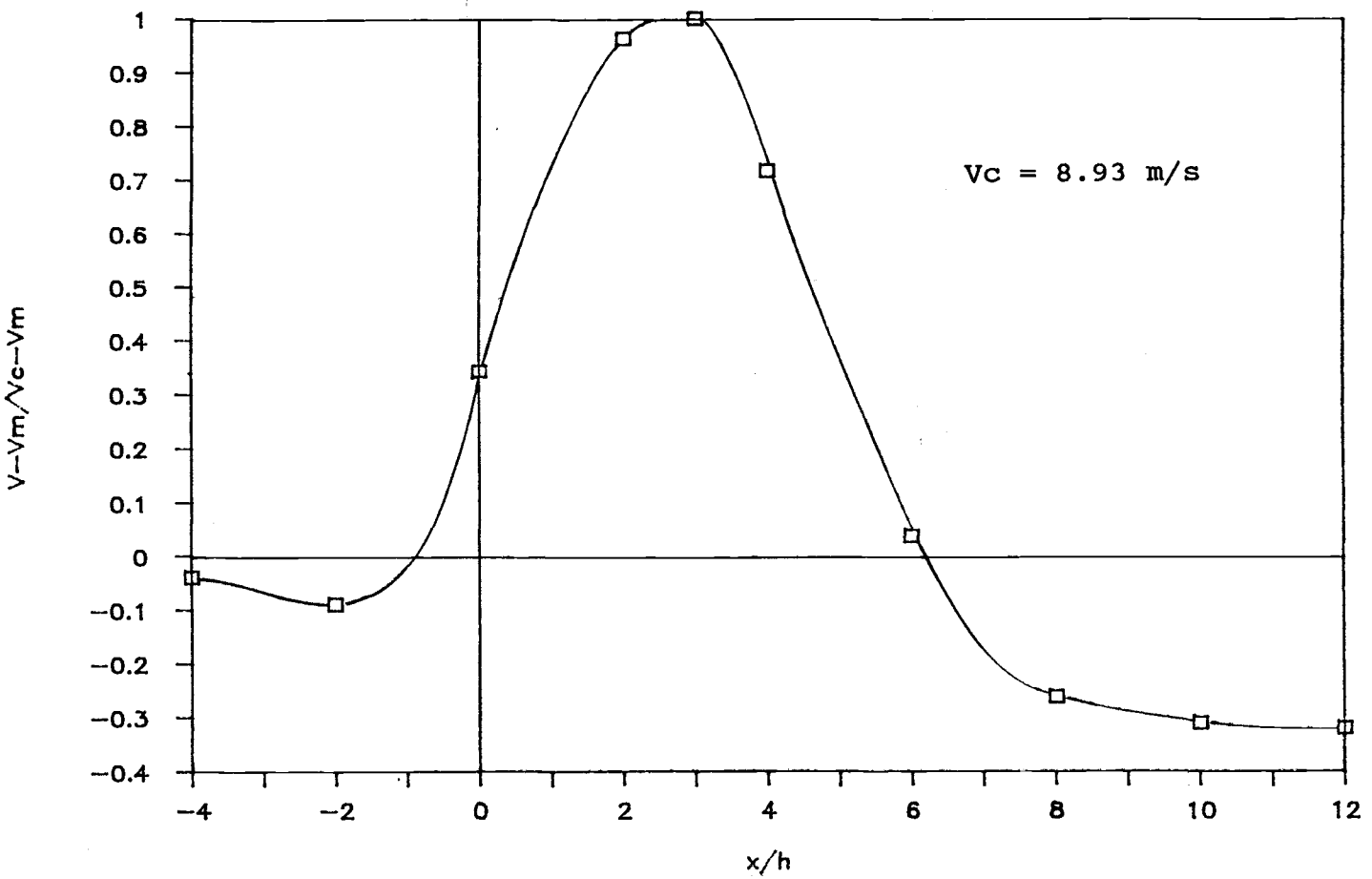

Figure A.19. Velocity distribution in jet cross-section for R = 6.2, $\Theta = 75^{\circ}$, y/h = 15

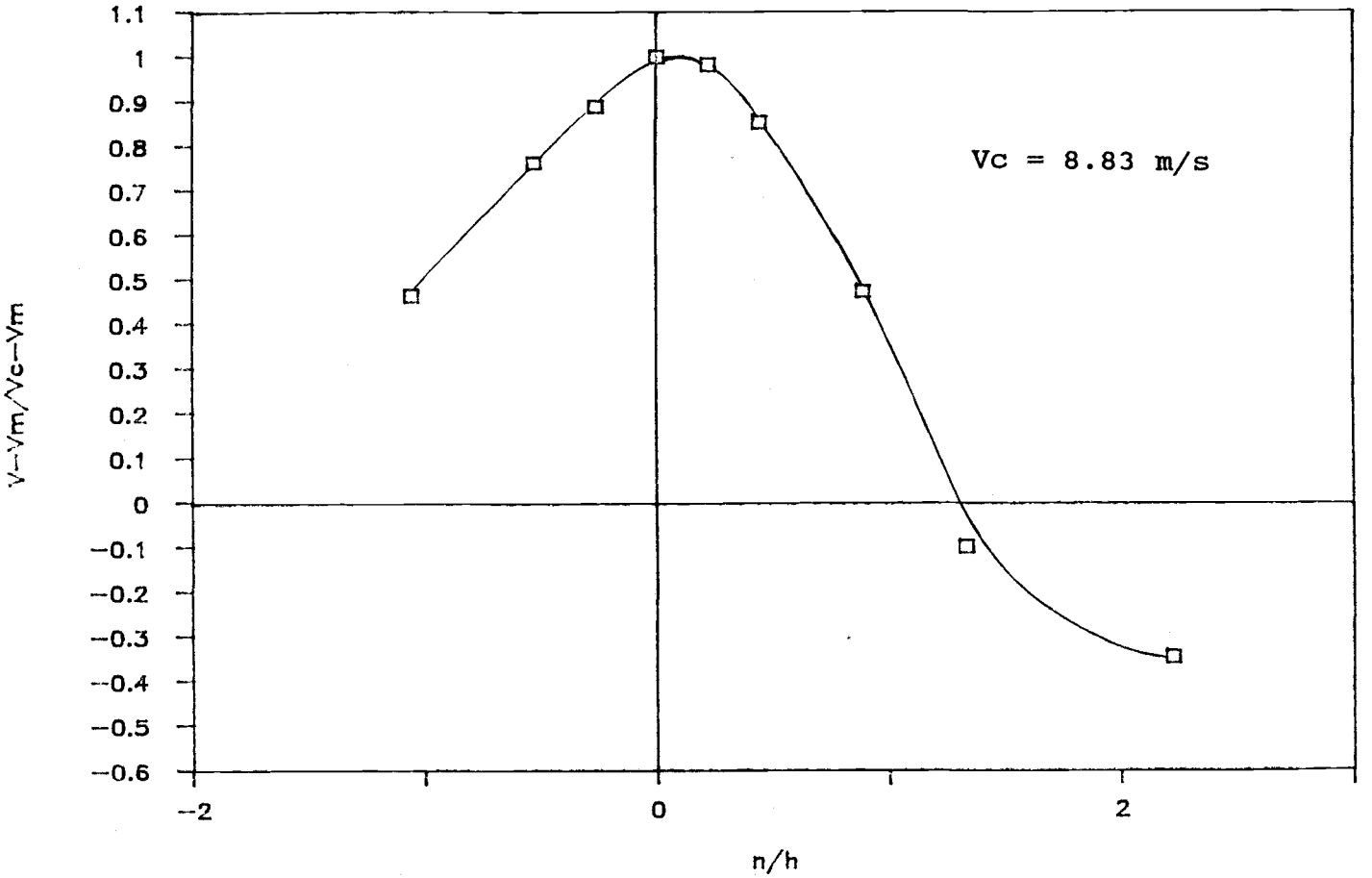

Figure A.20. Velocity distribution in jet cross-section for R = 6.2, $\theta = 60^{\circ}$, x/h = 10